TR-7
1967

Streamflow Forecasting Based on Statistical Applications and Measurements Made with Rain Gage and Weather Radar

M.D. Hudlow

Texas Water Resources Institute

Texas A&M University

STREAMFLOW FORECASTING BASED ON STATISTICAL APPLICATIONS AND MEASUREMENTS MADE WITH RAIN GAGE AND WEATHER RADAR

By

MICHAEL DALE HUDLOW

Water Resources Institute
Texas A&M University
August 1967

This investigation was supported in part by the Water Resources Institute, Project No. A-002-TEX, Texas A&M University, College Station, Texas, and the Office of Water Resources Research, Department of Interior.

FOREWORD

The primary emphasis in our investigation has been to gain a better understanding of the processes leading to precipitation and runoff in the State of Texas. This report has been the result of an effort by the author to utilize radar, rain gage, and streamflow information to develop "real-time" techniques for streamflow forecasting. Although data from the Little Washita River basin in Oklahoma were used in this study, the techniques are equally applicable to Texas.

All computer programs written in connection with this study are available in the Radar Meteorology Section of the Department of Meteorology.

ABSTRACT

Techniques for streamflow forecasting are developed and tested for the Little Washita River in Oklahoma. The basic input for streamflow forecasts is rainfall. The rainfall amounts may be obtained from several sources; however, this study is concerned with the possibility of utilizing weather radar and probabilistic simulation to obtain the rainfall input. Also, the feasibility of a radar, rain-gage combination is examined.

It is shown that quantitative estimates of runoff can be made from measurements taken with weather radar. In addition, accurate estimates of lag time can be made from radar observations. For a storm which is unevenly distributed over the watershed, it is demonstrated that a better estimation of lag time may be made from radar measurements than from measurements obtained from a sparse rain-gage network (1 gage/110 mi^2).

A technique for hydrograph synthesis which utilizes the Pearson type III function is developed. The use of the Pearson function for hydrograph synthesis constitutes a valuable tool for streamflow forecasting. Since this method of hydrograph synthesis is adaptable to the digital computer, the "time factor," which is so important for river forecasts, can be shortened.

A stochastic model (which incorporates a sixth-order Markov chain) for rainfall-runoff simulation is developed. Monte Carlo techniques are coupled with the stochastic model to yield frequency histograms of hydrograph-peak discharges and corresponding lag times. A model such as the one developed in this study could be coupled with radar observations to provide a probabilistic forecast of streamflow--shortly after rainfall commencement.

ACKNOWLEDGMENTS

The research upon which this report is based has been supported by Project No. A-002-TEX, Water Resources Institute, Texas A&M University, Dr. E. T Smerdon, Director, and the Office of Water Resources Research, Department of Interior. Dr. R. A. Clark, Department of Meteorology, is the Principal Investigator for this project which is a study of "The Morphology of Precipitation and Runoff in Texas."

Credit is due the Agricultural Research Service, Chickasha, Oklahoma, Mr. M. A. Hartman, Director, for furnishing rainfall and streamflow data. Radar data were furnished by Mr. K. E. Wilk, Radar Meteorologist, and Dr. E. Kessler, Director, National Severe Storms Laboratory, ESSA, Norman, Oklahoma. Additional streamflow data were provided by the Geological Survey, Oklahoma City, Oklahoma, Mr. A. A. Fischback, Jr., District Engineer.

TABLE OF CONTENTS

LIST OF FIGURES

LIST OF TABLES

LIST OF SYMBOLS

a,c	regression coefficients for Pearson's equation
a_i	area for the i^{th} subarea of the watershed
A,B	constants in Z-R relationship
API	antecedent precipitation index (in.)
A_t	the total area for the portion of the watershed that experiences rainfall excess
b_t	constant in t^{th} term of API equation
β	the deviation of a from the trial a which was used for the origin of the Taylor series expansion
c_n, c_o	new and old estimates in Newton's method for the numerical solution of equations
C	constant in radar equation
C_o, C_1, C_2	routing coefficients
d	raindrop diameter
d_m	maximum raindrop diameter
D,W	denote dry and wet periods for rainfall
$\underline{D}_t$	daily rainfall for t^{th} day used in API computation (in.)
Δt	routing interval
e	2.71828....
e_i	rainfall excess (runoff) for i^{th} subarea of watershed
E	rainfall excess (in.)
$f(\ )$	function designation
Γ	denotes Gamma function

I_i	mass inflow of water to i^{th} subarea of watershed
k	lag period for serial correlation
K	conversion factor to relate AREA in in.
K_{si}	storage coefficient for i^{th} subarea of watershed (hr)
ln	natural logarithm
L	length of flow path
Lg	lag time (hr)
m	complex index of refraction
n_i	number of raindrops in the i^{th} class interval
N	length of time series (hr)
O_i	mass outflow of water from i^{th} subarea of watershed
P	probability
P_r	hydrograph period of rise (hr)
$\overline{Pr}$	power received by radar
π	3.14159....
Q	hydrograph discharge (cfs)
Q_p	peak discharge of hydrograph (cfs)
Q_7	discharge for the seven hydrograph points fit to the Pearson function (cfs)
r	slant range to the radar target
r_k	serial-correlation coefficient for lag k
R	rainfall rate (mm/hr)
$\overline{R}$	average rainfall over an area for a storm (in.)
R^*	mass flux of water through a unit surface

ρ_w	density of water
s	error sum of squares
S	slope of flow path
S_i	storage of surface runoff for i^{th} subarea of watershed
t	time (day or hr)
t_{ci}	mean-travel time required for water from the i^{th} subarea to reach the gaging site
T	time (hr)
T_c	time of concentration (hr)
T_p	period of rise of the hydrograph minus the time elapsed between the beginning and the centroid of the rainfall excess (hr)
Tr	duration of rainfall excess (hr)
v	residual-damping factor
V_t	terminal fall speed of water droplet
w	vertical air speed
W	number of subareas within the watershed
W_{50}, W_{75}	hydrograph width at 50 and 75 per cent of the peak discharge (hr)
X_t	any discrete variable at time t; in this study X designates hourly rainfall amounts
Z	reflectivity factor (mm^6/m^3)
$Z_{1-\alpha}$	standardized-normal variate corresponding to the significance level α

C H A P T E R I

INTRODUCTION

General

Hydraulic structures such as dams can prevent or reduce damages caused by flooding. However, lack of suitable dam sites and/or economic constraints make the control of floods impractical in many instances. In such cases river forecasts provide an alternative means of reducing both flood damage and loss of life. If a flood forecast is issued in sufficient time to allow people, animals, and property to be evacuated, countless lives and dollars may be saved. The Office of Hydrology, Weather Bureau, Environmental Science Services Administration is the agency responsible for issuing such forecasts. Up-to-date forecasts are maintained for more than 1600 points on our nation's rivers.

The Bureau's forecasts are needed not only when floods threaten but are used daily by many major industries. The forecast provides streamflow information needed for such activities as shipping, production of hydroelectric power, crop irrigation, reservoir operation, manufacturing, and fish and wildlife management. In addition, river forecasts can provide indispensable knowledge

for pollution control. The greatest war on water pollution in history is under way in our nation. From a knowledge of the volumetric flow of a stream, discharge of municipal and industrial wastes can be regulated to keep stream pollution within safe limits.

Because of the importance of the "time factor," the most efficient techniques for the preparation and dissemination of forecasts must be utilized. The weather radar's capabilities of spatial and temporal coverage and its speed of data collection represent enormous possibilities for hydrologic work.

Hydrologic Use of Weather Radar

As a result of research during and immediately following World War II, radar was found to provide excellent indications of precipitation occurrence and storm movement. Shortly thereafter, it became apparent that the amount of energy returned to the radar generally increases as the rainfall rate increases. Tarble (1957) has enumerated the ways in which radar can serve the hydrologist. Because of its measurement capabilities, radar can aid in determination of storm duration, direction and speed of storm movement, temporal and spatial distribution of the rainfall, and antecedent conditions, as well as quantitative precipitation measurement. Complete coverage of

a watershed provides a decisive advantage of radar over the rain gage. In addition, the radar can allow the hydrologist to make a river forecast shortly after rain cessation, where it might take hours to collect enough rain-gage data for an accurate forecast.

The procedure developed in this study incorporates all the information mentioned above obtainable by radar. The speed and direction of storm movement are indirectly displayed by the storm duration and the temporal and areal distribution of the rainfall. The temporal distribution of rainfall can affect the rate of infiltration and, therefore, the quantity of runoff and the hydrograph peak or peaks of discharge. The spatial distribution of the rainfall can affect factors, used in hydrograph synthesis, such as lag time[1] and storage delay time.[2] Antecedent conditions can provide the hydrologist with an indicator of the soil moisture at the onset of the storm. The higher the soil moisture, the greater the runoff for a given amount of precipitation.

Nordenson and Richards (Chow, 1964, p. 25-99) have

---

[1]Lag time is defined for this study as the time from the centroid of rainfall excess to the centroid of the runoff hydrograph.

[2]Storage delay time is the time required for runoff from some portion of the watershed to reach the gaging site. Lag time is an average storage delay time.

pointed out that one of the basic problems in river forecasting lies in the collection and processing of the basic data. A flood warning received too late to permit evacuation of life and property is of no value. Therefore, for a radar to operate effectively as a forecast tool the data must be remoted to a river forecast center in real time.[3] Can rainfall data, measured by radar, be processed and remoted in real time? Kessler (1966) reported that techniques for processing and communicating radar data are not yet refined to the point where timeliness of reports and economy of operation are appropriately combined. However, it is believed that a satisfactory solution to this problem is within the foreseeable future.

Quantitative Precipitation Forecast

Nordenson and Richards (Chow, p. 25-109, 1964) mention the possible use of precipitation forecasts for streamflow predictions. In watersheds where the hydrograph period of rise is extremely short, river forecasts based on observed rainfall are of little value and precipitation forecasts must be used. For any watershed it would be advantageous if the hourly rainfall for an entire

---

[3]Real time is defined by Teague (1966) as a time period of no more than 30 min between rainfall occurrence and arrival of the processed precipitation data at a river forecast center.

storm could be forecast shortly after rain begins. However, the forecast models developed to date normally utilize large-scale vertical motion and some parameter of atmospheric moisture (e.g., precipitable water in an atmospheric layer). One such model has been developed by Harley (1965). Models of this type are strictly for simulations on a macroscale and in most instances fail to furnish the detail needed for streamflow forecasts. A portion of this study was devoted to the development of a probabilistic model which can be used for rainfall-runoff prediction.

Objective and Scope of Study

The objective of this study is to investigate and develop techniques which can be utilized for streamflow forecasting. The basic input is amounts of rainfall. The rainfall amounts may be obtained from any source; however, this study is concerned with the possibility of utilizing weather radar and probabilistic simulation to obtain the rainfall input.

Since, as mentioned above, the "time factor" is of an essentiality, all procedures are designed for adaptation to a digital computer. The forecast product is a hydrograph. A technique is perfected for describing the hydrograph by the Pearson type III function. In addition,

a runoff-routing procedure is utilized for hydrograph synthesis. Since the radar is superior to a sparse network of rain gages for determining the areal distribution of the rainfall excess and corresponding storage-delay times, it was believed that the feasibility of a runoff-routing procedure should be examined.

Falling within the scope of this study is the development of a Markov chain model for the prediction of hourly precipitation. The model is coupled with other relationships and Monte Carlo techniques to yield frequency histograms of hydrograph-peak discharges and corresponding lag times.

A study made by Teague (1966) is unique since it represents an attempt to correlate radar data with runoff. Teague made a comparison between rainfall measured by radar and runoff. The present study carries Teague's work further since it represents an attempt to use radar to estimate precipitation, in a temporal, spatial, and quantitative sense, as the input for hydrograph synthesis. The analyses and case studies are performed for the Little Washita River in Oklahoma.

CHAPTER II

DEVELOPMENT AND PROCEDURES

Source and Selection of Data

General. The watershed selected for investigation in this study is the experimental watershed comprising the drainage area for the Little Washita River in Oklahoma. The watershed is maintained by the Soil and Water Conservation Research Division, Agricultural Research Service (ARS), Chickasha, Oklahoma. The Little Washita basin was chosen because of the ample data available from rain-gage, radar, and stream-gage observations. The ARS maintains a dense network of recording rain gages on the Little Washita. The National Severe Storms Laboratory (NSSL), Environmental Science Services Administration (ESSA), Norman, Oklahoma operate a WSR-57 radar which scans the watershed. The WSR-57 radar has a wavelength of 10 cm. Radiation at this wavelength suffers negligible attenuation, even in the heaviest rainfall. Wilson (1964) has shown that the accuracy of the WSR-57 radar decreases appreciably beyond 60 n mi. The NSSL radar is within 45 n mi of the ARS watershed and thus falls within the criterion of 60 n mi set by Wilson. From the above discussion it becomes apparent that this combination of

weather radar and instrumented watershed offers excellent opportunities for hydrologic research.

Fig. 1 depicts the Little Washita basin and the ARS rain gage network. Each of these gages is a weighing-type, recording rain gage. The numbers indicate the identifying number assigned to each gage by the ARS. The locations of various Weather Bureau (WB) rain gages, which were used in the analyses, also are shown in Fig. 1.

The Little Washita River is a tributary of the Washita River, and lies south of the main stream. It flows generally eastward to join the main stream near Ninnekah, Oklahoma. Average discharge for the Little Washita is approximately 40 cfs (ft^3/sec). The maximum discharge on record of 30,000 cfs, which was estimated from flood marks, occurred in May 1949. Periods of zero flow are observed in some years.

The 210 mi^2 drainage area of the Little Washita River consists of Reddish Prairie and Cross Timber areas (see United States Department of Agriculture yearbook, 1957). Less than 50 per cent of the area is in cultivation; a large per cent is in open grass land. Principal crops are small grain and cotton.

Although the Little Washita watershed offers excellent opportunities for hydrologic research, a slight drawback exists in its use for a study of this type.

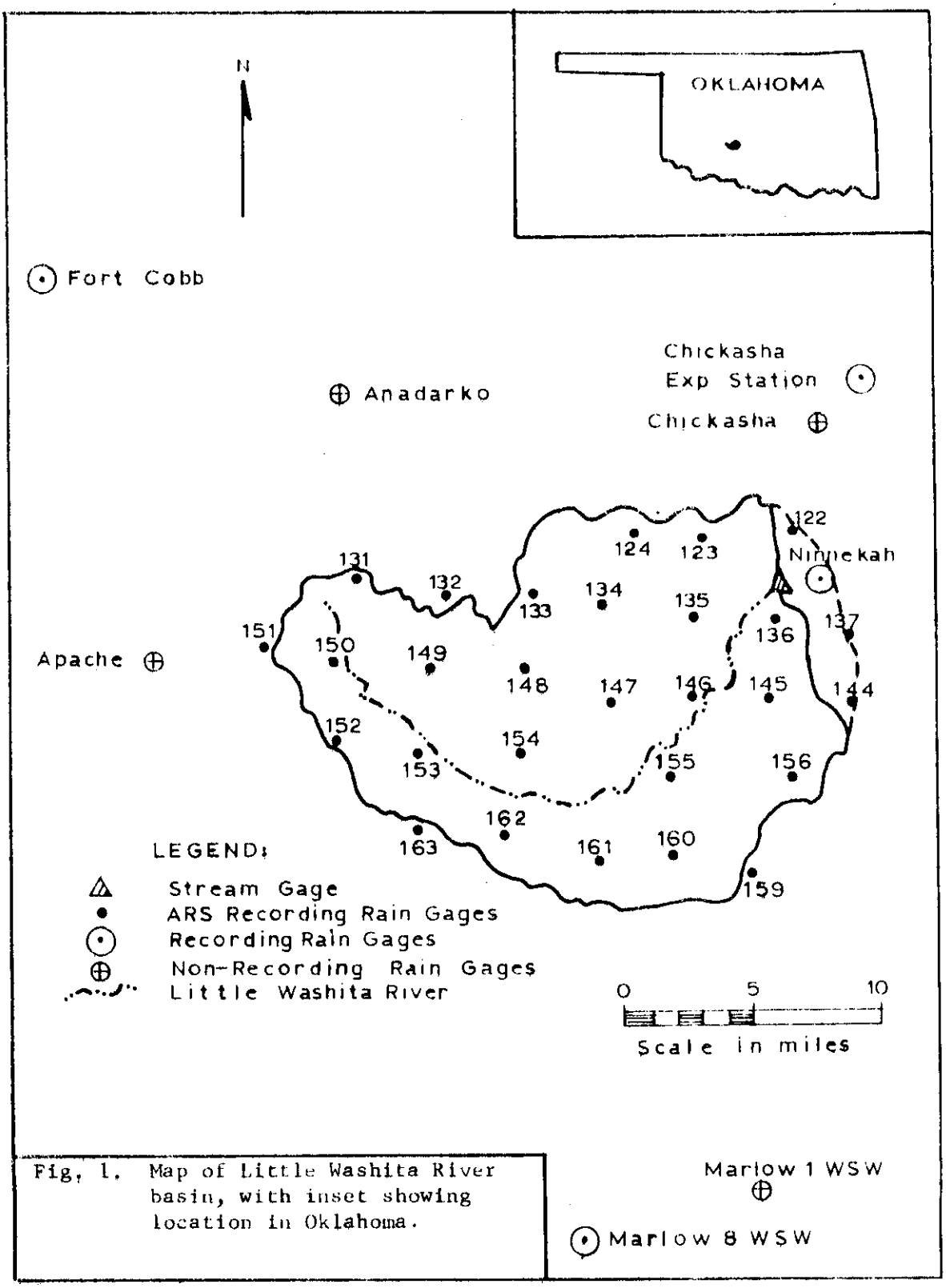

Fig. 1. Map of Little Washita River basin, with inset showing location in Oklahoma.

Extensive conservation practices are being employed on the watershed. For example, 21 per cent of the drainage area is controlled by farm ponds. ARS hydrologists are studying the effects of man-made conservation measures on streamflow. While such conservation measures act to increase infiltration and reduce erosion, an accompanying reduction in surface runoff will occur. For a "highly conserved basin" the reduction in surface runoff can be appreciable (see Hartman et al., 1967). It is felt that the conservation practices employed on the Little Washita basin acted to reduce the magnitude of the runoff events. For the 7 yr of record (1959-1965) considered for analyses, the largest runoff event selected is 7040 cfs, the next largest is 3800 cfs, and over 70 per cent of the events selected had peak discharges of less than 2000 cfs (see Table 1). The 7040 cfs event represents a discharge of 33 cfs per mi^2, while the remainder of the events represent much smaller amounts. Obviously, equations developed for streamflow forecasting from the runoff events described above cannot be used, justifiably, for runoff prediction of large magnitude. However, while the relationships developed for this study are not derived from storms of great magnitude, the techniques presented appear applicable directly to flood forecasting.

Rainfall. The ARS has maintained a dense network

Table 1. Average rainfall for watershed, duration of rainfall excess, runoff, peak discharge of surface hydrograph, lag time, and antecedent precipitation index for Little Washita basin, 1959-1965.

Storm No.	Date	R(in)	Tr(hr)	E(in)	Q_p(cfs)	Lg(hr)	API(in)
1	5/26/59	3.25	4.0	0.550	7040	7.4	0.252
2	7/1/59	2.15	2.0	0.042	750	9.3	0.101
3	6/4/61	1.18	1.0	0.069	865	9.8	0.228
4	9/13/61	4.33	2.5	0.178	1230	17.8	0.100
5	4/28/62	0.37	1.0	0.024	730	3.0	0.254
6	5/26/62	1.96	1.0	0.064	1080	9.7	0.229
7	6/2/62	2.70	2.0	0.177	3800	9.3	0.672
8	9/15/62	1.49	1.0	0.084	1885	11.0	0.086
9	10/28/62	1.60	2.0	0.062	1150	9.2	0.021
10	7/11/63	0.77	1.0	0.003	315	1.0	0.000
11	7/13/63	1.14	1.0	0.025	1265	2.4	0.149
12	4/3/65	0.25	1.0	0.012	535	1.5	0.009
13	5/26/65	1.52	1.0	0.037	960	4.8	0.051
14	6/2/65	0.90	1.0	0.025	500	5.7	0.121
15	8/28/65	1.19	1.0	0.055	2650	2.4	0.056
16	8/28/65	0.59	1.0	0.073	1710	6.6	0.306
17	8/31/65	0.72	1.0	0.037	1320	2.7	0.522
18	10/18/65	1.34	1.0	0.007	235	2.1	0.007

of approximately 20 rain gages on the Little Washita basin since 1963. In addition, there are four recording and four nonrecording WB rain gages, within reasonable proximity of the watershed (see Fig. 1), with periods of record in excess of 10 yr. All rainfall data used in the development of the forecasting procedures were extracted from WB records. It is realized that appreciable errors can result in analyses performed with the use of a sparse network of rain gages. However, analyses were performed with the WB rain gages for two reasons:

1. A hydrologist who develops a procedure for streamflow prediction (such as the one presented in this study) normally will have at his disposal only a sparse network of rain gages and no radar data. Therefore, the results of this study should not be biased by using an abnormal rain gage network or radar coverage for the analyses. The equation for prediction of runoff (Eq. 11, developed below) can be revised as analyses performed with the aid of radar coverage become available.
2. ARS rain-gage records for the Little Washita basin were not available prior to 1963; however, one-half the storms analyzed occurred prior to

1963. In addition, radar coverage was available for selected events.

The dense network of ARS rain gages is used later in this study for comparison with results synthesized by the procedures set forth.

Streamflow. Streamflow data are available through August 1963 for a stream gage maintained by the Geological Survey 0.5 mi north of Ninnekah, Oklahoma. Streamflow data since September 1963 are from a gage maintained by the ARS 2.2 mi farther upstream. The channel control is sandy and shifting in nature, and is unstable at low stages. A total of 18 storms was selected for analysis. The storms were chosen with a distribution of peak discharges from 235 to 7040 cfs (see Table 1). Four additional storms were selected for the case studies described later in this chapter.

Radar. As mentioned above, a WSR-57 radar maintained by NSSL scans the Little Washita watershed. Kessler (1966) describes the measurement and processing of the radar information as follows:

1. Photographs are made of the radar PPI display while the antenna scans continuously.
2. The resulting photographs are digitized and the data punched on IBM cards with the aid of

chart-reading "analog to digital conversion" equipment (Gray and Wilk, 1965).

3. The cards are processed by a computer program and assembled on magnetic tape (Kessler and Russo, 1963).
4. Digitized distributions of rainfall are calculated and output by computer.

A total of 6400 grids is used to depict the radar scope for the digitized output. Digitized distributions of rainfall over the watershed for the four case studies were provided by NSSL.

Data Analyses

General. Rainfall-runoff analyses were performed for a total of 18 storms. The storms were analyzed to determine:

1. The average rainfall over the basin for the entire storm.
2. The temporal distribution of average rainfall for the basin.
3. The surface runoff.
4. Losses (rainfall minus runoff).
5. The duration of the rainfall excess.
6. The peak discharge of the surface hydrograph.
7. The lag time.

A large portion of these analyses was achieved by Johnson (1967). Johnson's work was initiated partially for the purpose of furnishing this study with a satisfactory procedure to aid in the prediction of storm losses from radar observations.

Rainfall. The average rainfall over the basin for the entire storm, as well as the temporal distribution of average rainfall, was determined by Thiessen-polygon weighting (see Linsley, Kohler, and Paulhus, 1958, p. 36). In some instances isohyetal maps of total rainfall were prepared. The isohyetal maps were used as a tool for assessing the areal distribution of the storm.

In instances where rain gages of the nonrecording type were utilized, the temporal distribution of rainfall for the gage was determined by the mass-curve technique (Shands and Brancato, 1947). This technique yields an estimate of the time distribution of rainfall for a nonrecording gage based on the record of a nearby recording gage. The procedure involves the assumption that the same fractional amount of the total rainfall will occur in the same fractional period of the storm duration for both gages.

The duration of the rainfall excess comprises the time for which rainfall exceeds losses. This duration is determined by applying a constant loss rate to the

temporal distribution of average rainfall to yield the observed runoff.

Runoff. A computer program was prepared to separate the surface-runoff hydrograph from the ground-water hydrographs for the 18 storms. In addition, the computer program was designed to compute the surface runoff by the trapezoidal rule and to locate the centroid of the runoff volume. The subtraction of the ground-water flow involved the assumption that the base width of the surface hydrograph is always equal to five-time-the-period-of-rise, $5\ P_r$. A base width of $5\ P_r$ was adopted to ensure consistency between analyses and the hydrograph synthesis procedure described below (see Hydrograph synthesis with the Pearson type III function). Because ground-water discharge in the Little Washita is normally very small (generally less than 30 cfs), the procedure adopted for the ground-water separation is not critical. Fig. 2 illustrates the manner in which the hydrograph separation occurred. Some of the parameters derived from the rainfall-runoff investigations are used later in this chapter for regression analyses. The storm and hydrograph parameters are listed in Table 1.

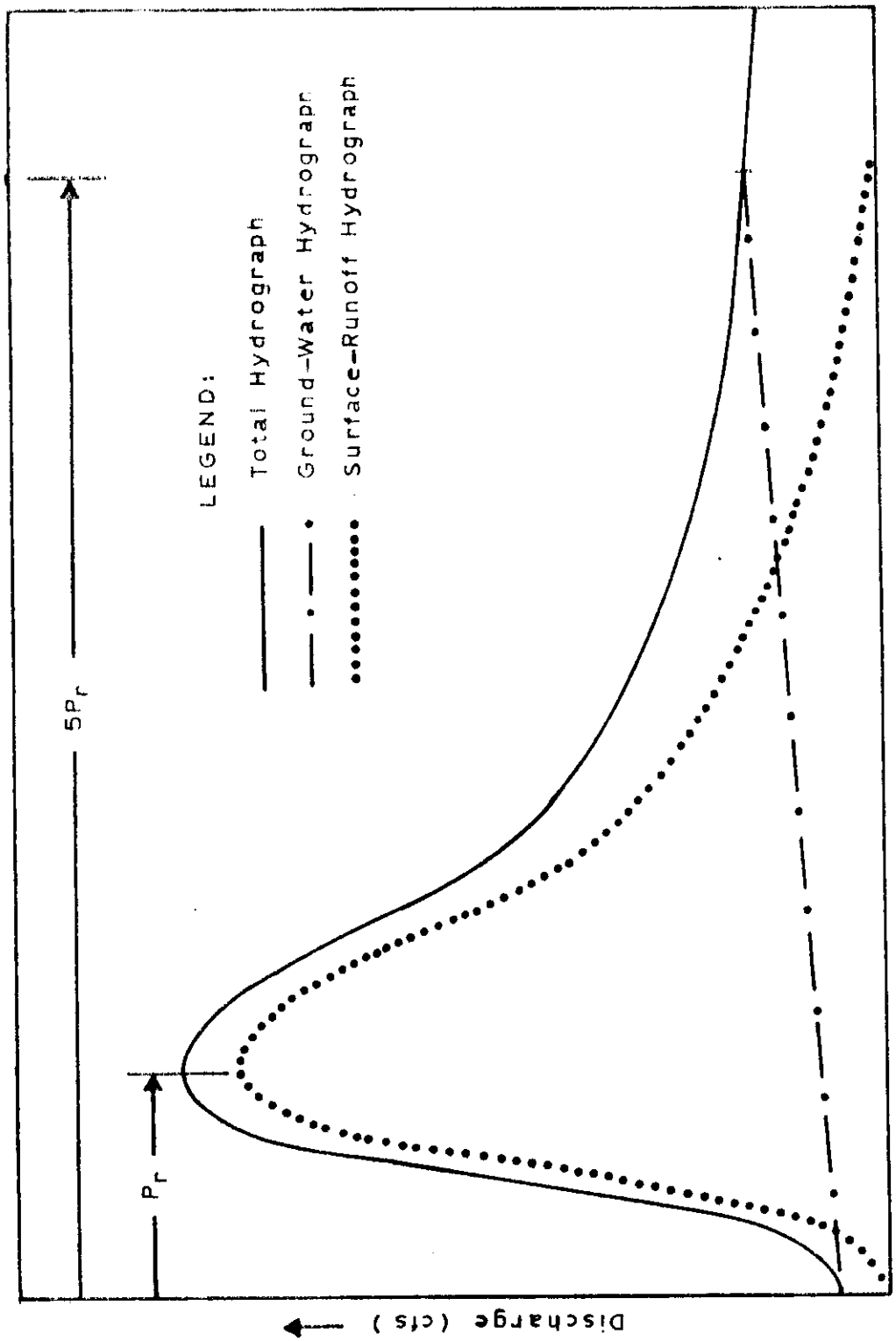

Fig. 2. Illustration of the method used to separate the ground-water hydrograph from the total hydrograph.

Quantative Measurement of Rainfall by Radar

According to the Rayleigh theory of scattering, the average power received from a volume of spherical particles, when the diameter of the particles is small compared to the wavelength of the incident radiation, is given by

$$\overline{Pr} = C|K|^2 \sum_{Vol} n_i d_i^6 / r^2 \quad , \tag{1}$$

where n is the number of drops in the i^{th} class interval of mean diameter, d; r is the slant range to the target; $K = (m^2-1)/(m^2+2)$, where m is the complex index of refraction; C is a constant which depends on the radar hardware; and $\overline{Pr}$ is the average returned power. By definition

$$Z = \sum_{Vol} n_i d_i^6 \quad , \tag{2}$$

where Z is called the reflectivity factor or simply reflectivity. Therefore, Eq. 1 can be written

$$\overline{Pr} = C|K|^2 Z / r^2 \quad . \tag{3}$$

Rearrangement of Eq. 3 yields

$$Z = \frac{\overline{Pr}\, r^2}{C|K|^2} \quad . \tag{4}$$

When reflectivity is evaluated from Eq. 4 with measured values of $\overline{Pr}$ and r^2, it is referred to as the "equivalent reflectivity factor." The "equivalent reflectivity factor" will, in general, vary from the theoretical reflectivity factor due to observational errors and departure from Rayleigh theory.

From physical considerations the mass flux, R^*, of water substance through a unit surface may be expressed as

$$R^* = \frac{\pi \rho_w}{6} \int_o^{d_m} n d^3 (V_t - w) \delta d \ , \qquad (5)$$

where ρ_w is the density of water; V_t is the terminal velocity; w is the vertical air speed; n is the number of drops within the drop interval δd; and d_m is the maximum drop diameter. By dividing both sides of Eq. 5 by ρ_w, the expression reduces to a rainfall rate,

$$R = (\pi/6) \int_o^{d_m} n d^3 (V_t - w) \delta d \ , \qquad (6)$$

where R is rainfall rate.

Eq. 6 can be integrated exactly provided realistic values can be obtained for the drop size distribution and the relative vertical velocity. Since these parameters are highly dependent on the mechanism producing the

precipitation, attempts have been made to elude these complexities by utilization of empirically derived Z-R relationships. However, as might be expected, the Z-R relationships vary considerably with precipitation type. Clark and Moyer (1966) have discussed the variability of Z-R relationships with storm characteristics (drop-size distribution and vertical velocity).

Numerous attempts have been made to relate Z and R. Since R is proportional to d^3 and Z to d^6 an equation of the form,

$$Z = AR^B \tag{7}$$

is suggested, where B should be approximately 2.0 and A some constant. However, A and B have been found to vary considerably with the type of precipitation (see Battan, 1959, p. 56). Values of A have been observed to range from 15 to 600 for rain and upward to 2000 for snow. Although B does not have as large a variation, a range of 1.2 to 2.9 has been reported. A slight revision of the equation proposed by Marshall and Palmer (1948) is the most frequently used Z-R relationship, i.e.,

$$Z = 200R^{1.6} , \tag{8}$$

where Z is in mm^6/m^3 and R in mm/hr. Imai (1960) has

pointed out that Eq. 8 strictly applies only to an average drop-size distribution and to the normal situation of continuous rain. However, as mentioned by Battan (1959, p. 55), many of the Z-R relationships that have been derived produce results similar to those from Eq. 8 within a practical range of drop sizes. The accuracy that can be expected from the use of a Z-R relationship increases with an increase of the area and time over which the rainfall is averaged.

There have been several attempts to develop techniques for selection of an appropriate Z-R relationship for a particular storm. Jones (1966) has discussed the possibility of obtaining better Z-R relationships by bracketing the precipitation into three types: thunderstorms, rainshowers, and continuous rain. As stated by Jones, an over-all increase in accuracy of up to 20 per cent can be obtained by such bracketing. However, the obvious difficulty lies in differentiating between thunderstorms and rainshowers from radar observations. A recent study by Wilson (1966) involved an examination of computer-derived statistics of radar patterns (average echo intensity, intensity variance, pattern bandedness, orientation of echo bands, and average echo length and width) to determine if a correlation exists between the statistics and the storm-to-storm variation of the Z-R

relationship. Because of the small sample considered, Wilson reached no definite conclusions concerning this approach. However, the author believes that such an approach offers great possibilities.

Since a satisfactory technique for selecting a Z-R relationship commensurate with a storm has not been perfected and since Eq. 8 is commonly used and characterizes an average situation, Eq. 8 was adopted for this study. The digitized distributions of precipitation furnished by NSSL for this study were prepared from computations based on Eq. 8.

Discussion of error. The errors that can result from the use of an inappropriate Z-R relationship represent only a portion of the possible errors that may occur in quantative-precipitation measurement by radar. The following uncertainties exist:

1. The radar data are themselves undertain by about $\pm$ 3 db (see Clark and Dooley, 1965, p. 122).
2. The rainfall sampled by the radar beam may not fill the radar beam completely.
3. Information concerning the rainfall distribution at the surface is sought; however the radar beam samples aloft. The height, at which

the radar beam samples, depends on atmospheric conditions and distance from the radar site.

4. The rainfall sampled aloft may be moved horizontally by the wind and partially evaporated before it arrived at the surface.

Most of these uncertainties become increasingly important when the rain varies significantly over short distances. Improved instrumentation and advanced techniques for data collection, processing, and communication will reduce the magnitude of these uncertainties. While rainfall measurement by radar, at the present state of the science, lacks preciseness, the radar does possess two inherent advantages:

1. The weather radar's spatial coverage makes it superior to a sparse network of rain gages for assessing the areal distribution of rainfall. Assessment of the areal distribution of the rainfall is necessary for an accurate prediction of lag time. This fact will be demonstrated in later discussions.
2. The radar's capability for remote coverage enables it to take measurements where rain-gage installations are impossible or economically

infeasible (e.g., over lakes, mountainous areas, or desolate areas).

Combination of radar and rain-gage data. Kessler (1966) has suggested, because of the variability of the Z-R relationship, that the measurement of rainfall by radar should be aided by rain gages in scattered locations. Until satisfactory techniques are developed for inferring the Z-R relationship for a particular storm, the radar, rain-gage combination appears the most feasible alternative. Kessler (1966) also has stated that additional study is needed to assess the number of rain gages needed for radar, rain-gage measurement. One such study recently has been performed by Huff (1966). Huff has used rain-gage measurements from one area to calibrate the radar equation for use in an adjacent area.

Since rain-gage transponders are now feasible, it is felt that an increased number of radar, rain-gage combinations may be installed in the future. Adjustment of areal averages of rainfall, measured by radar, from rain-gage data was considered for two storms in this study. One ARS rain gage (No. 147) located near the centroid of the Little Washita basin was used for the adjustment. The radar-measured rainfall in the radar grid containing rain-gage No. 147 was compared to the rainfall as measured by the rain gage. A factor was then determined for each

hour which when multiplied by the "radar rainfall" would give the observed "rain-gage rainfall." Each hourly factor was then applied to the other rainfall amounts (from radar) to yield an adjusted rainfall for the entire basin.

Antecedent Precipitation Index

Usually the amount of initial losses, which occur in the early portions of a storm, are a function of the initial soil-moisture conditions. However, in some areas this is not always the case; Schreiber and Kincaid (1967) found soil moisture to be a parameter that is rarely significant for runoff prediction for an experimental watershed in Arizona. The antecedent precipitation index (API) provides an indicator for initial soil-moisture conditions. Kohler and Linsley (Linsley, Kohler, and Paulhus, 1958, p. 171) propose the equation

$$API = b_1 D_1 + b_2 D_2 + \ldots\ldots b_t D_t \qquad (9)$$

where b_t is a constant less than unity, which decreases exponentially with t, and D_t is the amount of daily precipitation which occurs t days prior to the storm under consideration. The constant b_t, is given by

$$b_t = F^t \ , \qquad (10)$$

where F is a factor less than unity whose value will determine the number of preceeding days required in the API determination. The size of F depends on the soil-cover complex and evapo-transpiration, and therefore will vary somewhat with season. However, the most important factor influencing F appears to be the soil type (see Minshall, 1960, p. 22). For this reason a fixed value for F, for a reasonably homogeneous watershed, probably is adequate. A value of 0.85 for F was adopted for this study. This necessitates an antecedent period of 15 days for the API calculations.

It should be mentioned that other antecedent indicators might be used in association with the radar and operational forecasting. One possibility might be to use an equation analogous to Eq. 9 in which the precipitation amounts are replaced by the number of hours that precipitation is observed during each day. Such an API probably would not provide as good an index of the initial conditions of soil moisture; however, it offers one distinct advantage: it would be simpler to evaluate when utilizing radar data. In the use of weather radar for flood forecasting, it is quite possible that estimates of quantitative precipitation will not be made by radar, unless the storm is sufficiently large to represent a potential flood. However, all rainfall that occurs within a reasonable time span prior to the storm in question,

contributes to the initial soil moisture. Although the preceeding storms might not appear of sufficient magnitude to warrant a detailed analysis of quantative precipitation, it would be a simple matter to keep track of the number of hours that precipitation occurs over sub-regions of the watershed. API as defined by Eqs. 9 and 10 was used exclusively for this study.

Regression Analyses

Five equations, one for runoff prediction and four for hydrograph synthesis, were developed by the procedure of least squares. All five equations are highly significant statistically. Complete analysis of variance (ANOVA) tables are presented in Appendix B.

Runoff prediction. The equation developed for runoff prediction is the most critical of the five equations. For this reason it will be examined in greater detail than the other four. Runoff prediction is critical because a hydrograph can be determined adequately if the amount and distribution of the rainfall excess (runoff) is known. This fact will become apparent from later discussions.

Numerous variables may influence the quantity of runoff (rainfall-minus-runoff) resulting from a storm. Storm rainfall, antedecent precipitation, storm duration,

rainfall intensity, and time-of-the-year all may have an effect on the amount of runoff accompanying a storm. Various models involving these variables were examined. It became apparent readily that a non-linear equation would be required to predict adequately the runoff. A computer program was written to test the significance of each variable considered in the regression analysis. Storm precipitation was found to play a significant role, and no improvement was gained by including storm duration or intensity in the prediction model. The soil-cover complex of the watershed normally changes somewhat with season. For this reason the time of the year was considered as a possible factor for inclusion in the prediction equation for runoff. However, for the 18 storms considered in this study, there was no enhancement in the regression model due to time of the year.

The equation selected for runoff prediction includes storm precipitation and an index of initial soil-moisture (API). The "Cobb-Douglas" function was selected as the most appropriate model. The equation obtained is

$$E = 0.0961\bar{R}^{0.81}API^{0.357} , \qquad (11)$$

where $\bar{R}$ is the average rainfall for the storm in inches; API is the antecedent precipitation index, in inches; and E is the rainfall excess (runoff) in inches. For the

least-squares procedure the "Cobb-Douglas" function was linearized by a logarithmic transformation. Sharp et al. (1960) have pointed out that for many hydrologic variables (e.g., runoff) the assumption that the variance of the dependent variable does not depend on the values of the independent variables is not wholly justified. Therefore, a logarithmic transformation, which necessitates a multiplicity error-term, should make the use of multiple-regression analysis satisfactory for such hydrologic investigations.

A residual plot was constructed for Eq. 11 (see Fig. 3). This is a plot of $\overline{R}$ versus API with the residual (difference between observed and predicted runoff) labeled for each point. Also, the number of the storm is shown above each point. As can be seen from the residual plot, essentially all of the variability unexplained by Eq. 11 is the result of storm No. 1. The reason for this variability is not readily apparent. Since storm No. 1 produced the largest runoff of any of the 18 storms, this might suggest that the "Cobb-Douglas" function is inadequate for large-runoff events and that some different function might prove more suitable. However, from examination of the residual plot it becomes apparent that this is not the case for this sample. Storm No. 7 occurred with an API over twice as large

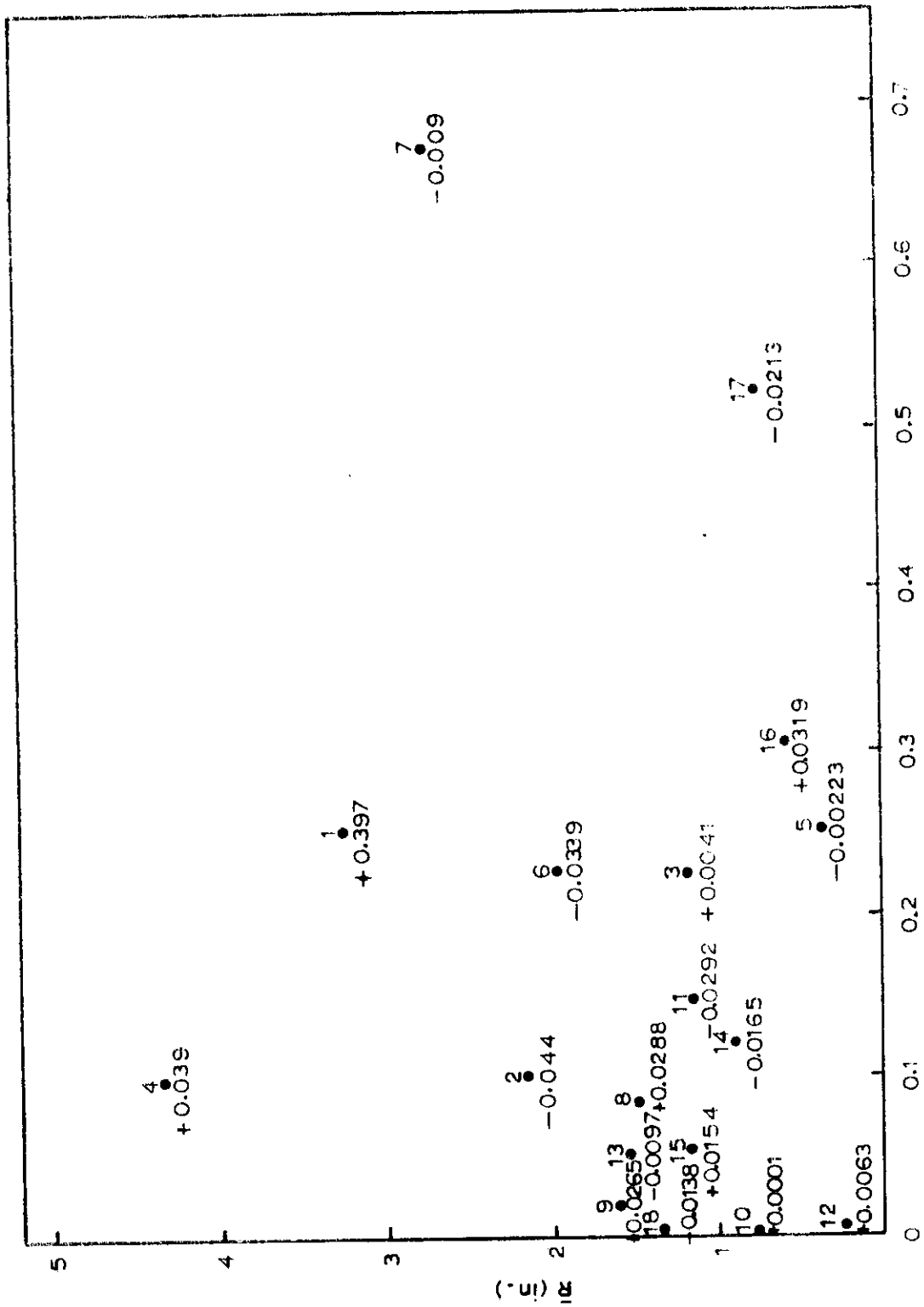

Fig. 3. Residual plot for Eq. 11.

and with a rainfall only slightly less than for storm No. 1; however, the runoff for storm No. 7 was approximately one-third that of storm No. 1. Storm No. 4 occurred with approximately one-fourth more rain than storm No. 1 and with an API appreciably less (but still of a moderate amount) than storm No. 1. However, as in the case of storm No. 7, the runoff from storm No. 4 was approximately one-third that of storm No. 1. The reason for this variance among runoff amounts (especially between storm No. 1 and storm No. 7) is not apparent. A variation between the soil-cover complex existing over the watershed for the different storms might account for some of the variability described above. But, from examination of Table 1 it is seen that storm No. 1 occurred on May 26 and storm No. 7 occurred on June 2. Although the two storms are for different years, the soil-cover complex should not vary appreciably, since both storms occurred at almost identical times of the year.

One possible improvement in Eq. 11 might have been achieved by considering antecedent precipitation longer than 15 days for the API calculations. Nonetheless, Eq. 11 satisfactorily predicted the runoff events of small magnitude for the case studies, while it appreciably under-estimated the one event of large magnitude used in the case studies.

The peak discharge of a hydrograph is a function of the areal distribution of the rainfall excess as well as the amount of runoff. As illustrated by the Soil Conservation Service (1957, p. 3.15-1), lag time may be thought of as an average travel time for the watershed.[4]

Hydrograph parameters. For a given storm the lag time is given by

$$Lg = \sum_{i=1}^{W} \frac{(a_i e_i t_{ci})}{A_t E} , \qquad (12)$$

where a_i is the area of the i^{th} subarea;[5] e_i is the rainfall excess for the i^{th} subarea; t_{ci} is the mean travel-time for the i^{th} subarea; A_t is the area for the portion of the watershed that experiences rainfall excess; E is the total runoff for the watershed; and W is the total number of subareas.

From the definition, Eq. 12, it is apparent that the lag time is a function of the areal distribution of the rainfall excess. Therefore lag time and total runoff

---

[4]Time of concentration is the time required for water to travel from the hydraulically most distant portion of an area of rainfall excess to the watershed outlet.

[5]For this study the watershed is divided into subareas bounded by the isochrones needed for evaluating Eq. 12 (see Fig. 4). A discussion of the techniques used for the construction of the isochrones is given in the section entitled Hydrograph Synthesis.

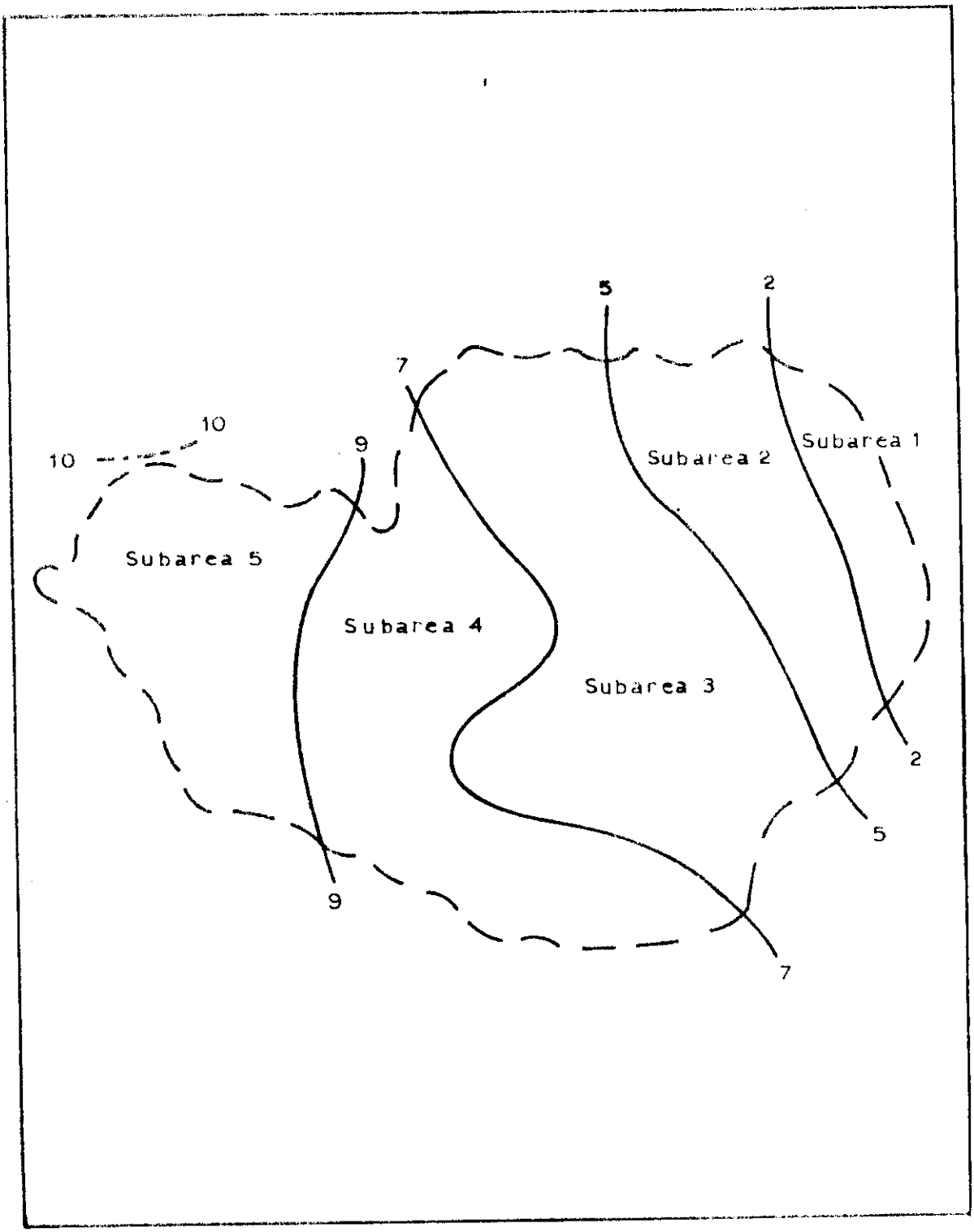

Fig. 4. Isochrones for the Little Washita (hr).

were used as the independent variables for the prediction of peak discharge. Once again, the "Cobb-Douglas" function was selected as the appropriate model. The resulting equation is

$$Q_p = 58460\ E^{0.944}/Lg^{0.642}\ , \qquad (13)$$

where Q_p is the peak discharge of the hydrograph in cfs; E is in inches; and Lg is in hours.

In order to establish the hydrograph period of rise, a relationship was sought between T_p and Lg where T_p is equal to the period of rise of the hydrograph minus the time elapsed between the beginning and the centroid of the rainfall excess. For any one watershed the ratio of T_p to Lg should be essentially constant because the hydraulic characteristics of most basins change inappreciably. Therefore, a linear relationship was assumed and a regression equation obtained by "least squares" for the T_p versus Lg data. Initially, the line was not required to pass through the orgin; however, the null hypothesis that the intercept equals zero was accepted. Next, a straight line passing through the orgin was derived. The resulting equation is

$$T_p = 0.823\ Lg\ , \qquad (14)$$

where both T_p and Lg are in hours.

In order to describe the complete hydrograph by the technique described in the following section, expressions for the width of the hydrograph at 50 and 75 per cent of the peak discharge must be derived. Since the shape of simple hydrographs for a given basin remain reasonably unchanging, a relationship should exist between the width of the hydrograph, at a fixed per cent of the peak discharge, and the period of rise. The hydrograph width should increase from a very small value, for an extremely short period of rise, to larger values, for longer periods of rise.

A plot on semi-logarithmic paper of the hydrograph width at 50 per cent of the peak discharge versus the period of rise revealed the relationship as exponential. The least-squares solution gave

$$W_{50} = 2.258e^{0.107P_r} , \qquad (15)$$

where W_{50} is the width of the hydrograph at 50 per cent of the peak discharge in hours, and P_r is the hydrograph period of rise in hours.

For the same watershed a relationship must exist between W_{75} (hydrograph width at 75 per cent of the peak discharge) and W_{50}. A direct relationship between W_{75} and W_{50} assures that the shape of the hydrograph

conforms to the characteristic shape for the watershed. A straight-line relationship with zero intercept was chosen as the appropriate model. The least-squares solution gave

$$W_{75} = 0.558W_{50} , \qquad (16)$$

where both W_{75} and W_{50} are in hours.

For a unit hydrograph (one producing 1 in. of runoff) in the Little Washita River basin Eqs. 15 and 16 yield results which are comparable to the hydrograph widths obtained from curves prepared by the Corps of Engineers (see Linsley, Kohler, and Paulhus, 1958, p. 206). However, unit hydrographs were not considered in this study and the hydrograph widths obtained vary appreciably from those which would be computed from the derivation of a unit hydrograph.

Hydrograph Synthesis

General. There are two fundamentally different techniques for hydrograph synthesis. The first of these techniques consists of estimating hydrograph parameters, usually peak discharge and some time parameter, from watershed and storm characteristics. From these two parameters and available information concerning the hydrograph shape, the remainder of the hydrograph can be

sketched. The second method involves routing of rainfall excess (surface runoff) through catchment storage to produce an outflow hydrograph of surface runoff for a catchment. Both approaches for hydrograph synthesis will be utilized in this study.

It is believed that the radar can offer decisive advantages over a sparse rain-gage network when used with either of the foregoing techniques. The radar can supply information concerning the temporal and areal distribution of the rainfall. This information will allow for an accurate evaluation of lag time. Therefore, the capability of the routing procedure to synthesize a complex hydrograph resulting from a non-uniform distribution of rainfall excess was examined.

The Little Washita watershed was divided into five subareas bounded by isochrones (see Fig. 4). Initially, it was thought that at least 10 subareas should be used. However, as can be seen from Fig. 4, hourly isochrones would be tightly packed in the lower portion of the watershed. This was largely a result of the basin configuration and tributary arrangement of the Little Washita. Therefore, it was decided that only five subareas would be used. The rainfall excess occurring over each subarea was determined in the same manner for both of the procedures of hydrograph synthesis. The average precipitation

and API for each subarea are used with Eq. 11 to predict the rainfall excess. The average precipitation for each subarea was assumed equal to an arithmetic average of the rainfall amounts, for the subarea, furnished by the NSSL radar or the ARS rain gages. Average API for each subarea was determined by weighting the API values from nearby WB rain gages. For operational forecasting, API could be evaluated from antecedent measurements made with radar.

Once the total rainfall excess has been determined for a subarea the temporal distribution of the rainfall excess may be estimated. This is accomplished by applying an average-loss rate to the hyetograph for the subarea to yield the computed runoff for each subarea.

Hydrograph synthesis with the Pearson type III function. From Eqs. 12, 13, 14, 15, and 16 and two additional relationships concerning the positioning of the hydrograph widths at 0, 50, and 75 per cent of the peak discharge, seven points on the hydrograph may be determined. The Corps of Engineers have suggested, as a guide for shaping the hydrograph, that the hydrograph widths at 50 and 75 per cent of the peak discharge should be positioned so that one-third of the width is placed to the left and two-thirds of the width to the right of the hydrograph peak. However, this research has indicated

that an allocation of four-tenths of the width to the left and six-tenths of the width to the right produces optimum results when the procedure outlined in Appendix A is used.

One other relationship is needed, this being a relationship for the base width of the unit hydrograph. Following the practice of the Soil Conservation Service and the Corps of Engineers, a base width of $5\ P_r$ was adopted.

The Pearson type III function was selected as the most appropriate mathematical function for fitting the seven points. This function can be written as

$$Q = Q_p(T/P_r)^a \exp[-(T - P_r)/c] , \qquad (17)$$

where Q is the discharge in cfs at any time T; T is the time in hours from the beginning of rainfall excess; Q_p is the peak discharge in cfs; P_r is period of rise of the hydrograph in hours; a is a dimensionless constant for a particular hydrograph; and c is a constant for a particular hydrograph, expressed in units of hours. Two iterative procedures are combined to solve for the c and a that give a least-squares fit of Eq. 17 to the seven points.

Hudlow (1966) has proposed the use of the Pearson

type III function, in the above capacity, and has developed a least-squares technique for fitting the Pearson function to the seven points. In that study the "goodness-of-fit" of the Pearson function to the seven hydrograph points was shown to be excellent. Since 1966, the author has improved the portion of the procedure that guarantees that the hydrograph will contain an area equivalent to the volume of runoff. This technique for fitting hydrograph data with the Pearson type III function is presented in Appendix A. The over-all scheme for hydrograph synthesis, with the Pearson type III function, is illustrated in Fig. 5.

Hydrograph synthesis by runoff routing. From an intensive study of routing procedures, Laurenson (1962) has concluded that a general procedure for runoff routing should provide for:

1. Temporal variations in rainfall excess.
2. Areal variations in rainfall excess.
3. Different elements of rainfall excess passing through different amounts of storage.
4. Catchment storage being distributed rather than concentrated.
5. A non-linear relationship between stream discharge and catchment storage.

Based on the study of 1962, Laurenson (1964) published a

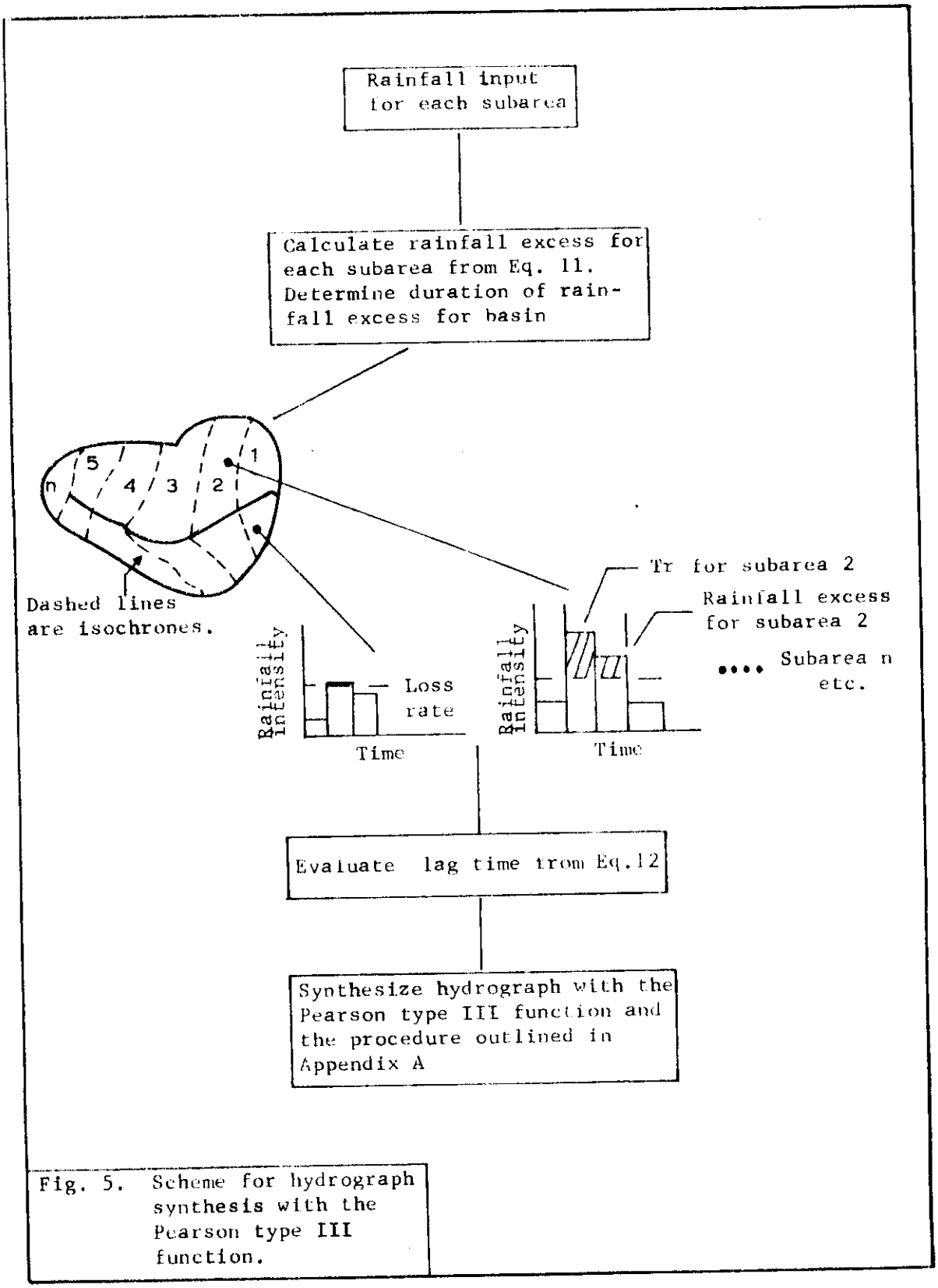

Fig. 5. Scheme for hydrograph synthesis with the Pearson type III function.

description of a procedure for runoff routing which provides for these five occurrences. His work was used as a guide for deriving the runoff-routing model adopted for this study. However, the procedure used in the derivation of the routing model differs in two respects from that of Laurenson:

1. Time of concentration, instead of lag time, was selected as the time parameter used in the isochrone construction. All travel times were considered a fraction of the time of concentration.
2. Identification of a possible non-linear relationship between stream discharge and catchment storage was accomplished from examination of concentration times, instead of lag times, for selected storms.

Laurenson implies that the relationship between stream discharge and catchment storage is generally non-linear. This means that the storage-delay time, for a given subarea, varies with the magnitude of the outflow from the subarea. If we assume that only prism storage exists (see Linsley, Kohler, and Paulhus, 1958, p. 227), the storage-discharge relationship may be expressed as

$$S_i = K_{si}(O_i)O_i \ , \qquad (18)$$

where S_i is the storage for the i^{th} subarea for a given outflow and K_{si} is the storage coefficient (storage delay time) for the i^{th} subarea; (O_i) indicates that the storage coefficient may be a function of the outflow.

The subareas used for the routing procedure are the same as those used for hydrograph synthesis with the Pearson type III function. The isochrones were constructed based on the assumption that travel time is proportional to

$$L/\sqrt{S} \ , \tag{19}$$

where L is the length of the flow path and S is the slope of the flow path. Such a relationship can be supported by the Chezy formula (see Chow, 1964, p. 7-23). The following steps were taken in the construction of the isochrones:

1. An average time of concentration was determined from hydrograph analysis of selected storms (see Johnstone and Cross, 1949, p. 229).
2. A large number of points were located on a topographic map of the watershed.
3. Travel times for each point were obtained from two applications of Eq. 19. The total travel time was assumed equal to the sum of the

travel times for overland flow and channel flow.

The isochrones are those shown in Fig. 4.

The fundamental equation used for runoff routing (mass continuity equation) can be expressed as

$$(I_1 + I_2)\frac{\Delta t}{2} - (O_1 + O_2)\frac{\Delta t}{2} = S_2 - S_1 , \qquad (20)$$

where I is inflow, O is outflow, here S refers to storage, and the subscripts 1 and 2 refer to the beginning and end of the routing period (Δt), respectively. Substitution for S_2 and S_1 from Eq. 18 yields

$$O_2 = C_o I_2 + C_1 I_1 + C_2 O_1 , \qquad (21)$$

where

$$C_o = C_1 = \Delta t/(2K_{s2} + \Delta t) ,$$

and (22)

$$C_2 = (2K_{s1} - \Delta t)/(2K_{s2} + \Delta t) .$$

Since C_o, C_1, and C_2 depend on K_{s2}, an iterative solution of the system of routing equations is required if K_{s2} is a function of O_2 (non-linear model).

Laurenson assumed that there exists a non-linear relationship between stream discharges and catchment storage if the lag time varies significantly with average

discharge for selected storms. However, an examination of the variability of T_c with Q_p appears to represent a more logical approach. This is because lag time is highly dependent on the distribution of the rainfall excess. For watersheds with areas larger than a few square miles, it becomes difficult to find storms that are evenly distributed over the basin. Nevertheless, the distribution of the rainfall excess is not a critical factor in the evaluation of the time of concentration.

Eight storms were selected for the determination of T_c (time of concentration). Fig. 6 is a plot of T_c versus Q_p for the Little Washita. There is no indication from this figure that a significant relationship exists solely between T_c and Q_p. Therefore, a linear routing model was adopted for this study. Since the model was assumed to be linear, the principle of superposition is applicable. Rainfall excess from each subarea was routed independently to the outlet, and the five separate outflows were combined.

Table 2 gives the storage coefficients for the five subareas used with the routing model.

Table 2. Storage coefficients for the Little Washita.

Subarea	1	2	3	4	5
K_{si} (hr)	1.0	3.5	6.0	8.0	9.5

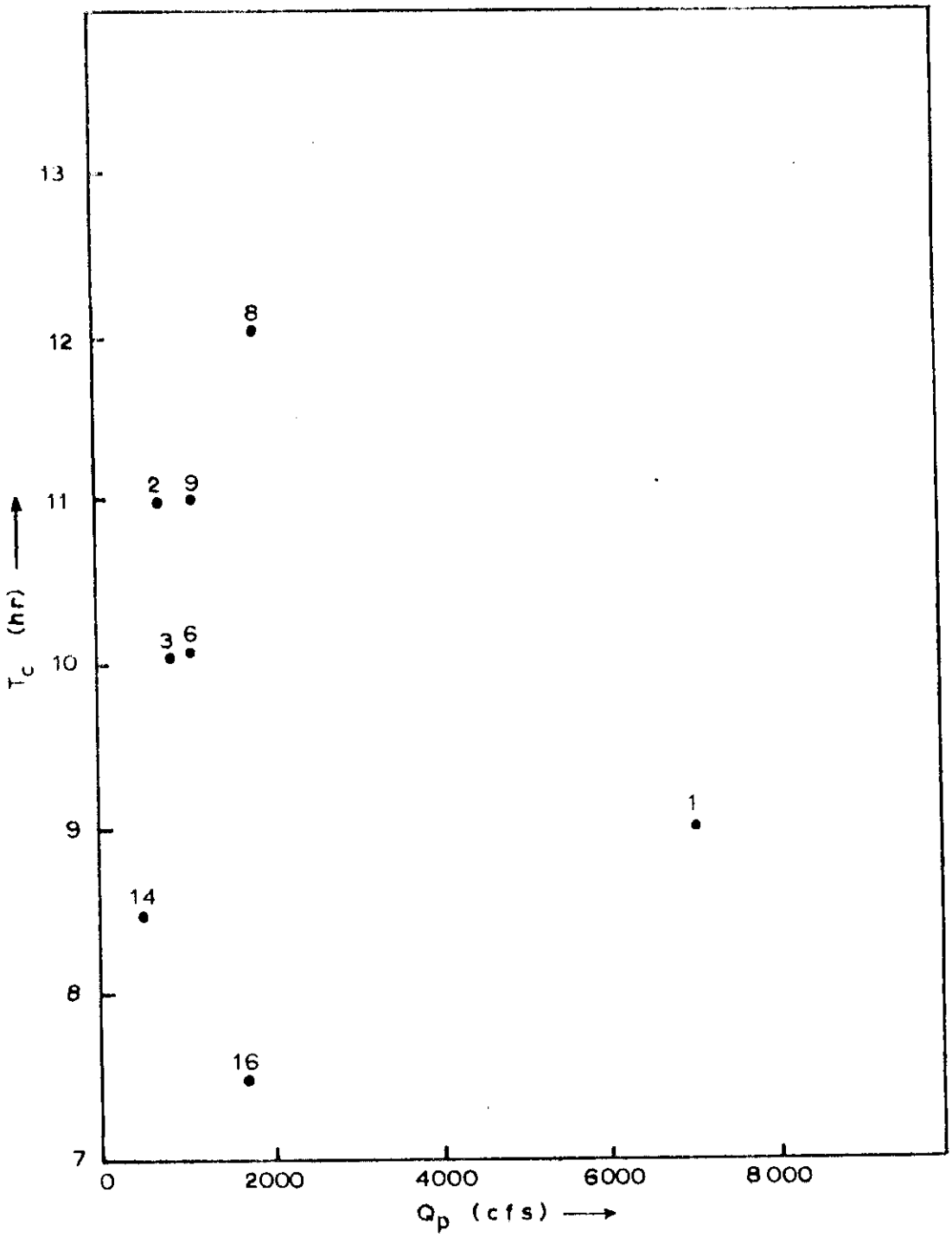

Fig. 6. Time of concentration versus peak discharge for the Little Washita.

Fig. 7 illustrates the scheme for hydrograph synthesis with the linear model for runoff routing.

Case Studies

General. Table 7 (which is presented in Chapter IV) lists the storms that were available for case studies. Average precipitation and runoff estimates were made, for each of these storms, based on rainfall measurements made with:

1. The complete ARS rain-gage network.
2. The NSSL radar.
3. Only two rain gages (ARS gages 137 and 151).

The estimates made from radar measurements then are compared to those derived from the dense ARS rain-gage network and to those based on a sparse rain-gage network (two ARS gages). Arithmetic averages were used to determine storm rainfall from the ARS rain-gage network and the NSSL radar-grid network. From results based on only the two ARS rain gages, areal averages of storm rainfall were estimated by Thiessen-polygon weighting. In all cases runoff was computed from Eq. 11.

In addition to the precipitation and runoff estimates that were made for the four storms listed in Table 7, two of the storms were selected for further study. Estimates of lag time and peak discharge were made and

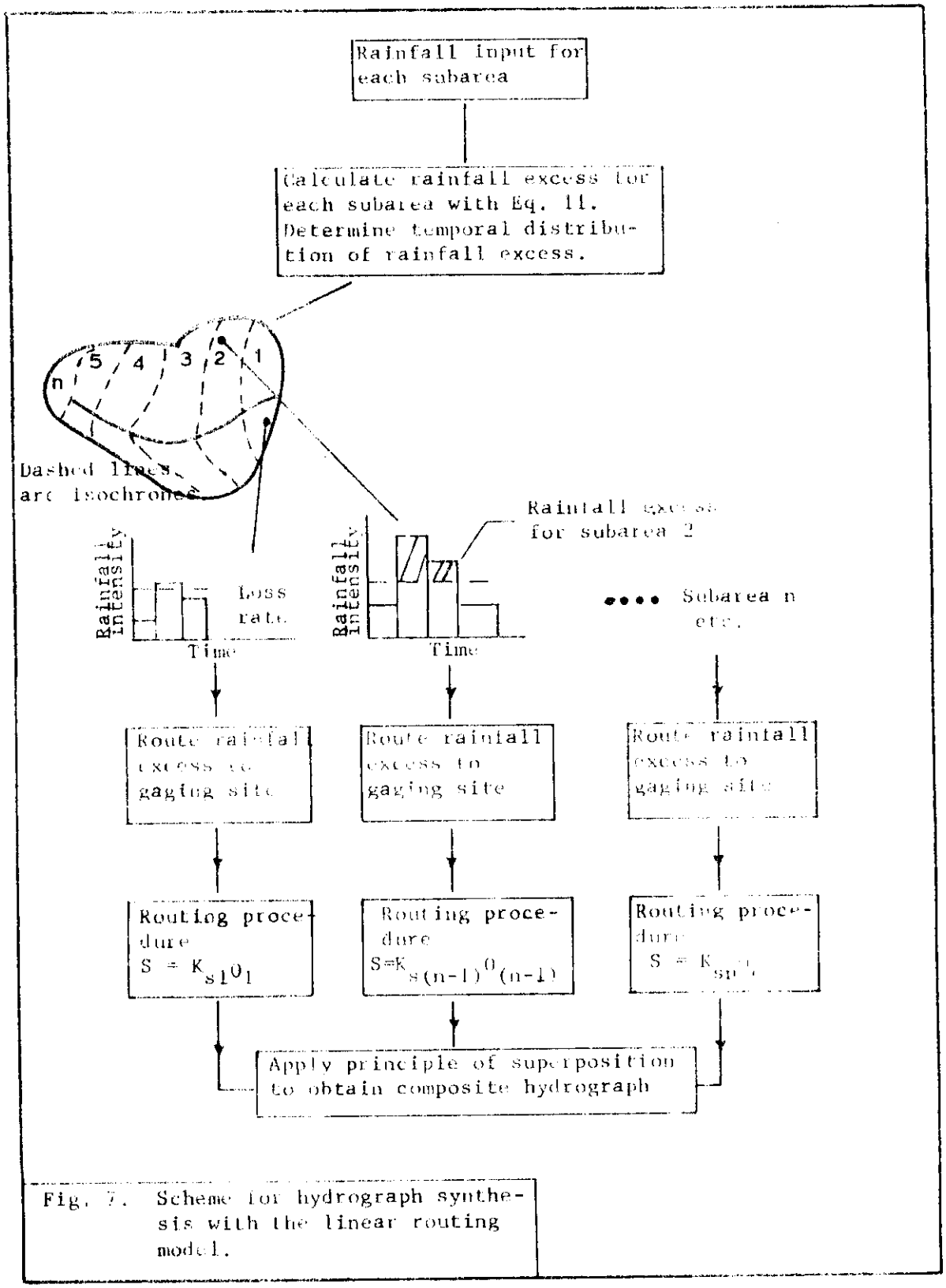

Fig. 7. Scheme for hydrograph synthesis with the linear routing model.

hydrographs were synthesized for storms 19 and 20. Also, the stochastic model was tested on these two storms. Storm 19 was, essentially, evenly distributed over the basin, while storm 20 was concentrated toward the upper portion of the watershed. Isohyetal patterns for storms 19 and 20 are presented in Fig. 8. Since storm 20 was unevenly distributed over the basin, it affords an excellent opportunity to examine the inherent advantage of the weather radar over a sparse rain-gage network, i.e., to depict the areal distribution of the rainfall.

It was decided that the radar, rain-gage combination would be used as another means of rainfall measurement for storms 19 and 20. These two storms allow examination of the feasibility of the radar, rain-gage combination for measurement of both uniform and uneven areal distributions of rainfall.

Hydrograph synthesis. Hydrographs were synthesized for storms 19 and 20, based on the various rainfall measurements discussed above, with the Pearson type III function. Also, since storm 20 is complex (two peaks), it was selected as the "test storm" for the routing model. Therefore, hydrographs were synthesized for storm 20 with the linear routing model as well as with the Pearson function. Comparisons are made between the predicted hydrographs and the observed hydrographs.

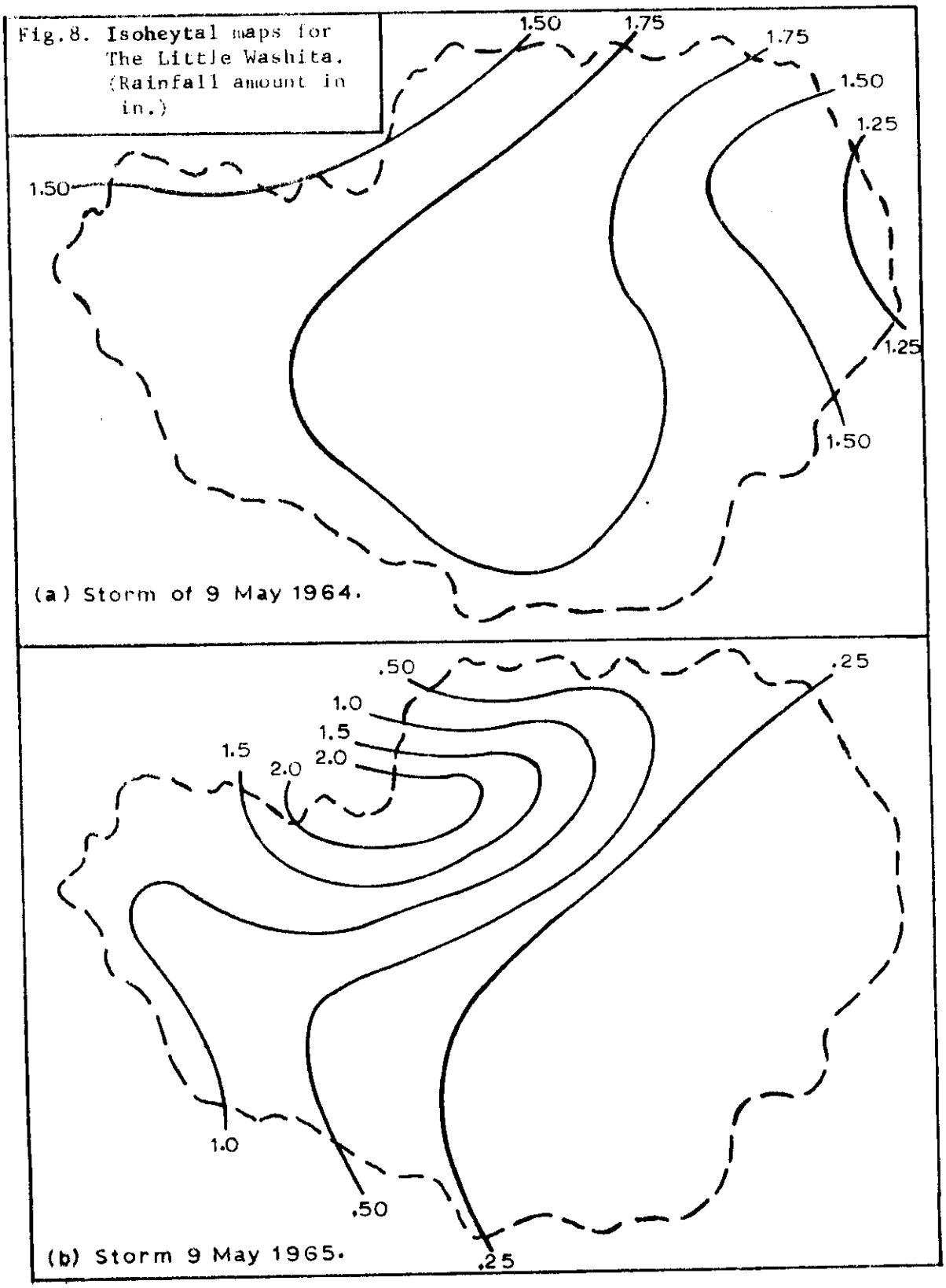

Fig. 8. Isoheytal maps for The Little Washita. (Rainfall amount in in.)

Rainfall-runoff simulation by stochastic model. The rains occurring with storms 19 and 20 were both associated with stationary fronts. The stochastic model developed in Chapter III was used with "synoptic type 3" (see Table 4) and rainfall-runoff forecasts were made for storms 19 and 20. The first hour of rainfall for storm 19 was assumed to be known, and a precipitation forecast for the subsequent 6-hr period was made. In the case of storm 20, three separate forecasts were made. The three forecasts were:

1. The first hour of the storm was assumed to be known and a precipitation forecast for the subsequent 6 hr was made.
2. The first 2 hr of the storm were assumed to be known and a precipitation forecast for the subsequent 6 hr was made.
3. The first 3 hr of the storm were assumed to be known and a precipitation forecast for the subsequent 6 hr was made.

The three forecasts for storm 20 were made for the purpose of disclosing any improvement in the runoff prediction by the addition of successive hours of "known" rainfall. The total rainfall (the "known" amount plus the forecast amount) was then used for the computations of runoff from Eq. 11.

CHAPTER III

STOCHASTIC MODEL FOR RAINFALL-RUNOFF SIMULATION

Rainfall Model

In recent years the term stochastic hydrology has received widespread usage. Stochastic hydrology is defined as the manipulation of statistical characteristics of hydrologic variables to solve hydrologic problems. One such stochastic technique involves the use of a Markov chain for the simulation of rainfall and/or runoff. A. A. Markov (1856-1922), a Russian probabilist, introduced the concept of a stochastic process known as the Markov process, or Markov chain (see Parzen 1960). In the classical sense, for a Markov process, the probability of a system experiencing a given state depends only on the knowledge of the state of the system at the immediately preceding time. However, in recent years it has become customary to consider stochastic processes with greater than first-order time dependencies as Markov chains. For example, if the existing state depends on the two immediately preceding times and corresponding states, such a process is called a second-order Markov chain. N^{th} order chains are defined similarly. If the existing state depends only on the immediately preceding

time and state, such a process is called a first-order Markov chain or simply a Markov chain. A first-order Markov chain can be said to exist if the

$$P(X_{t+1}|X_t,X_{t-1}, \ldots\ldots,X_1) = P(X_{t+1}|X_t) \ , \qquad (23)$$

where P denotes the probability of occurrence of the quantity within parentheses, X_t denotes the amount at time t, and the slash can be read as "given that." The set of probabilities for all states in the system forms what is called the matrix of transitional probabilities. The transitional probabilities define the chain (see Parzen, 1960). If the transitional probabilities are considered time dependent, the Markov chain is called homogenous or stationary. Once the transitional probabilities have been established, the discrete distribution can be synthesized by Monte Carlo (random) selection of the probabilities and corresponding amounts.

In order to justify the use of a Markov chain for depiction of the hourly rainfall process (hourly amounts are considered for this study), we must first establish that hourly precipitation is a non-random occurrence. Serial correlation coefficients are indicators of the non-randomness of a time series. The serial correlation coefficient is analogous to the product-moment correlation coefficient for two sets of data. If X_i and X_{i+k}

are considered as two sets of data, the k^{th}-order serial correlation coefficient is given by

$$r_k = \frac{\sum_{i=1}^{N-k} (X_i - \bar{X}_i)(X_{i+k} - \bar{X}_{i+k})}{\sqrt{\left(\sum_{i=1}^{N-k} (X_i - \bar{X}_i)^2 \sum_{i=1}^{N-k} (X_{i+k} - \bar{X}_{i+k})^2\right)}} , \qquad (24)$$

where the bar designates the mean and N is the length of the time series. For large samples a time series is random if $r_k = 0$ for all values of $k > 0$. However, for finite samples, computed values of r_k may differ from zero because of sampling error. Since N (number of hours of rainfall) is small for most storms, a test of significance for r_k must be made. Anderson (1942) has developed a test of significance for the serial correlation coefficient. For large samples ($N > 30$) a normal approximation yields the following formula for the single-tail significance points of r_1,

$$r_1 = \frac{-1 \pm Z_{1-\alpha}\sqrt{(N-2)}}{N-1} , \qquad (25)$$

where $Z_{1-\alpha}$ is the standardized normal variate corresponding to the significance level α. For small values of N or for $k \geq 1$, tables of significance points are presented by Anderson. Anderson's test of significance

for the serial correlation coefficient was adopted for this study.

Serial correlation coefficients for hourly rainfall were computed and correlograms were plotted for 100 storms occurring at Ninnekah, Oklahoma. A correlogram is a graphical representation of r_k versus k (lag). For the storms of sufficient duration to warrant significance tests for $k = 1$ $(N > 7)$, r_1 was almost always significantly different from zero. Generally for $k \geq 2$, r_k was found insignificant. The average correlogram, as computed from the ten longest storms $(N \geq 20)$, is shown in Fig. 9. Since r_1 is significantly different from zero, it can be concluded that the hourly rainfall process is a non-random occurrence for which the present state depends on the immediately preceding period. Fig. 9 shows r_k decreasing monotonically with increasing k and thus supports the autoregressive or Markov process.

Pattison (1965) has used a Markov-chain model for synthesizing hourly amounts of rainfall. Pattison's model was designed for use with the Stanford Watershed model (Crawford and Linsley, 1962); it has produced satisfactory results at several locations in California. Pattison (1964) observed some important features of the rainfall process; two of these are worth noting:

1. Most rainfall systems produce sporadic rain.

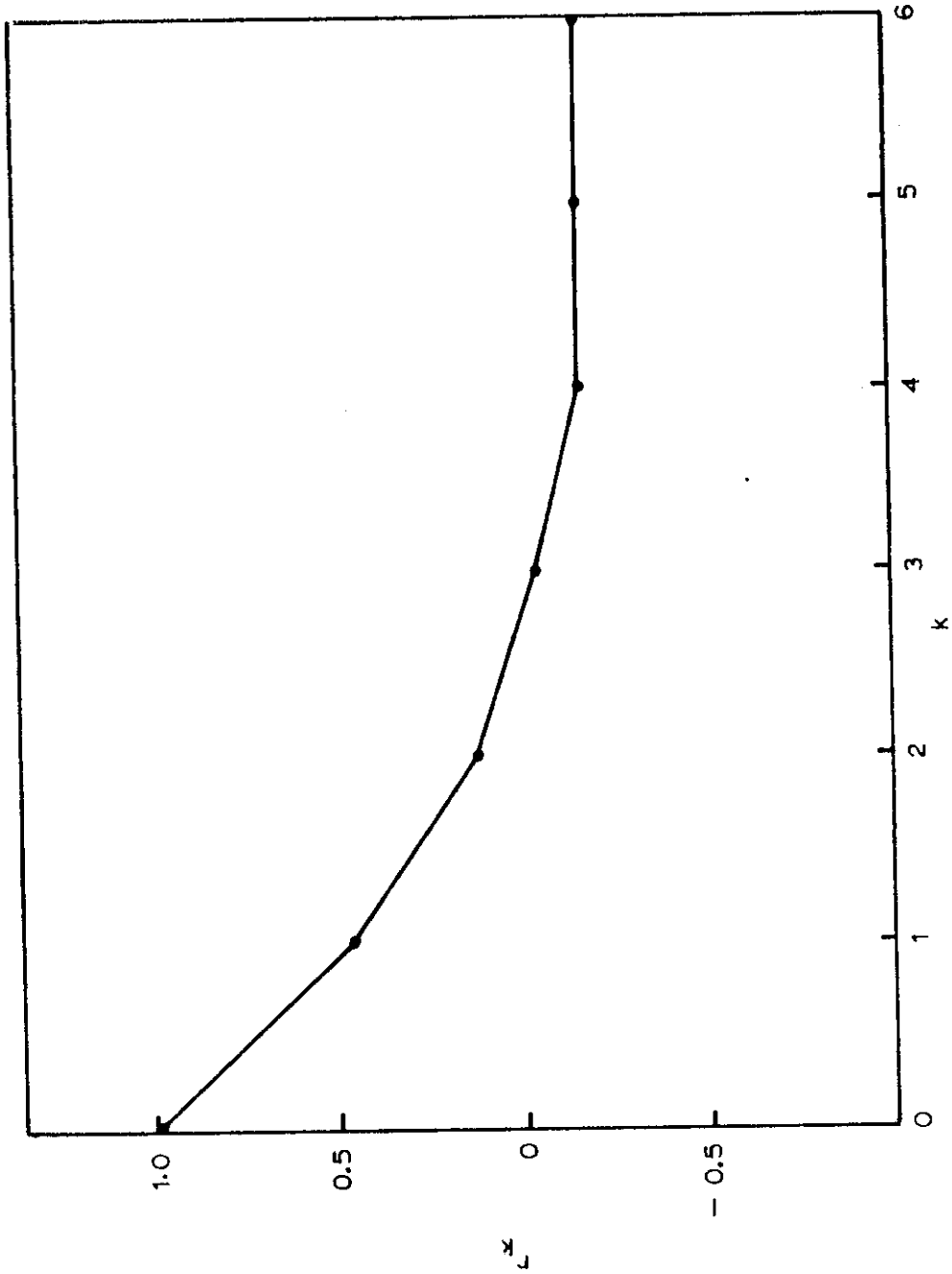

Fig. 9. Average correlogram of hourly rainfall at Ninnekah, Oklahoma.

2. The rainfall-producing process which exists at any given time is in a state which was achieved by the interaction of the conditions which existed during the immediately preceding period.

It is interesting to note that feature 2 is in exact agreement with results obtained from the serial correlation analysis above.

Pattison's model (1965) provides for inclusion of the dry hours which occur during sporadic rain storms. Pattison assumed the transition probabilities to be stationary within each month of the year but to vary from month to month. The Markov chain developed for this study differs basically in three respects from Pattison's:

1. Synoptic type replaces the month of the year for the stationary periods.
2. Diurnal persistence is considered during dry hours.
3. The model was derived for a different area.

Huddle (1967) has proposed a Markov-chain model and presented the transitional probabilities for the hourly rainfall process at Ninnekah, Oklahoma. The chain was derived from approximately 175 scattered months of hourly precipitation data from the periods 1940-1942 and 1949-1966. Huddle's work was initiated partially for the purpose of furnishing this study with a satisfactory rainfall

model. The model is used, as described below, to provide the precipitation input for runoff synthesis.

As illustrated above, the basic-synthesis procedure should involve the autoregressive or Markov process. Pattison (1964) has investigated the possibility of using a linear autoregression model of the first order. In this study the Markov chain has proved superior to the linear model. A non-linear autoregressive model might prove successful; however, a Markov chain coupled with Monte Carlo simulation offers greater flexibility.

The Markov chain proposed by Huddle, like Pattison's, consists of a primary and a secondary portion. The primary considers only first-order dependencies and is used exclusively during sequences of non-zero rainfall (wet hours). However, as soon as a dry hour is forecast the secondary portion of the chain, which considers sixth-order dependencies, must be adopted. The over-all simulation procedure involves an interplay between the primary and the secondary portions of the chain.

Because of the relatively short period of record available at Ninnekah, a restricted number of rainfall classes was considered. If too many classes were used, meaningful probabilities could not be assessed. In addition, the greater the number of classes, the greater the computational difficulties. A practical number had to

adopted which was compatible with the purpose of the model. Huddle selected ten classes for the hourly amounts of rainfall (see Table 3). The hourly process is recovered in the simulation scheme by selecting the mean rainfall for the class. The mean rainfalls for the classes, as determined from the 175 months of useful record, also are presented in Table 3.

Since the synoptic situations which can produce rainfall in Oklahoma differ in type, it was decided that the stationary periods adopted for this study would consist of six synoptic types. As indicated by Huddle, the synoptic situation which occurs is somewhat related to the time of the year, i.e., the two are not independent. It is likely that utilization of both variables would yield improved results. This was not possible for this study because only 15 yr of data were available. Any further division of the data into separate groups would have resulted in frequencies so low as to make it impossible to calculate meaningful probabilities.

Hiser (1956) has separated the precipitation observed in Illinois into six synoptic types. Hiser's classifications are: (1) cold front; (2) warm front; (3) stationary front; (4) squall line; (5) warm air mass; and (6) cold air mass. Consideration of synoptic situations which produce precipitation in Oklahoma led to

Table 3. Classes of hourly amounts of rainfall and mean rainfall for the classes.

Class	Amount	Mean Amount for Class
1	0.00	0.00
2	0.01	0.01
3	0.02-0.03	0.024
4	0.04-0.06	0.048
5	0.07-0.10	0.087
6	0.11-0.20	0.150
7	0.21-0.30	0.254
8	0.31-0.40	0.352
9	0.41-0.70	0.542
10	>0.70	1.000

the conclusion that these six types constitute a valid scheme of classification.

Huddle assigned each day of rainfall, throughout the 175 months of acceptable record at Ninnekah, Oklahoma, to one of the above synoptic types. The procedure admittedly was somewhat subjective, but, as stated by Huddle, in perhaps one-half of the cases a decision could be made with very little doubt of accuracy. The summer months contributed a large number of clear-cut occurrences of type 5 (warm air mass) rainfall, while the winter months logically contributed a large number of type 1 (cold front) occurrences. Decisions were difficult for the cases where a front was more or less stationary in the area. In such cases, type 3 was sometimes appropriate, although types 1, 2, and 5 also had to be considered.

An example of the first-order transitional probabilities is presented in Table 4. These are the probabilities for synoptic type 3 (stationary front).

An acceptable rainfall model must be capable of reproducing, for sporadic rain, the dry hours dispersed among the wet ones. For this purpose a secondary portion of the Markov chain was developed. The decision of whether an additional dry hour or hours should be forecast, following a dry hour prediction from the first-order

Table 4. First-order transitional probabilities for synoptic type 3 (stationary front).

State During Hour (t-1)	State During Hour (t)									
	1	2	3	4	5	6	7	8	9	10
1	-----	0.247	0.209	0.138	0.130	0.117	0.054	0.013	0.050	0.042
2	0.490	0.245	0.132	0.063	0.025	0.020	0.013	0.006	0.006	0.000
3	0.404	0.192	0.199	0.089	0.021	0.055	0.020	0.020	0.000	0.000
4	0.318	0.150	0.121	0.050	0.112	0.103	0.028	0.009	0.009	0.000
5	0.295	0.032	0.147	0.158	0.168	0.137	0.042	0.021	0.000	0.000
6	0.228	0.026	0.096	0.123	0.150	0.219	0.079	0.035	0.009	0.035
7	0.089	0.054	0.054	0.018	0.179	0.232	0.179	0.036	0.071	0.088
8	0.071	0.071	0.107	0.143	0.036	0.143	0.250	0.107	0.036	0.036
9	0.200	0.080	0.080	0.120	0.040	0.040	0.160	0.160	0.000	0.120
10	0.037	0.037	0.037	0.074	0.037	0.333	0.074	0.185	0.075	0.111

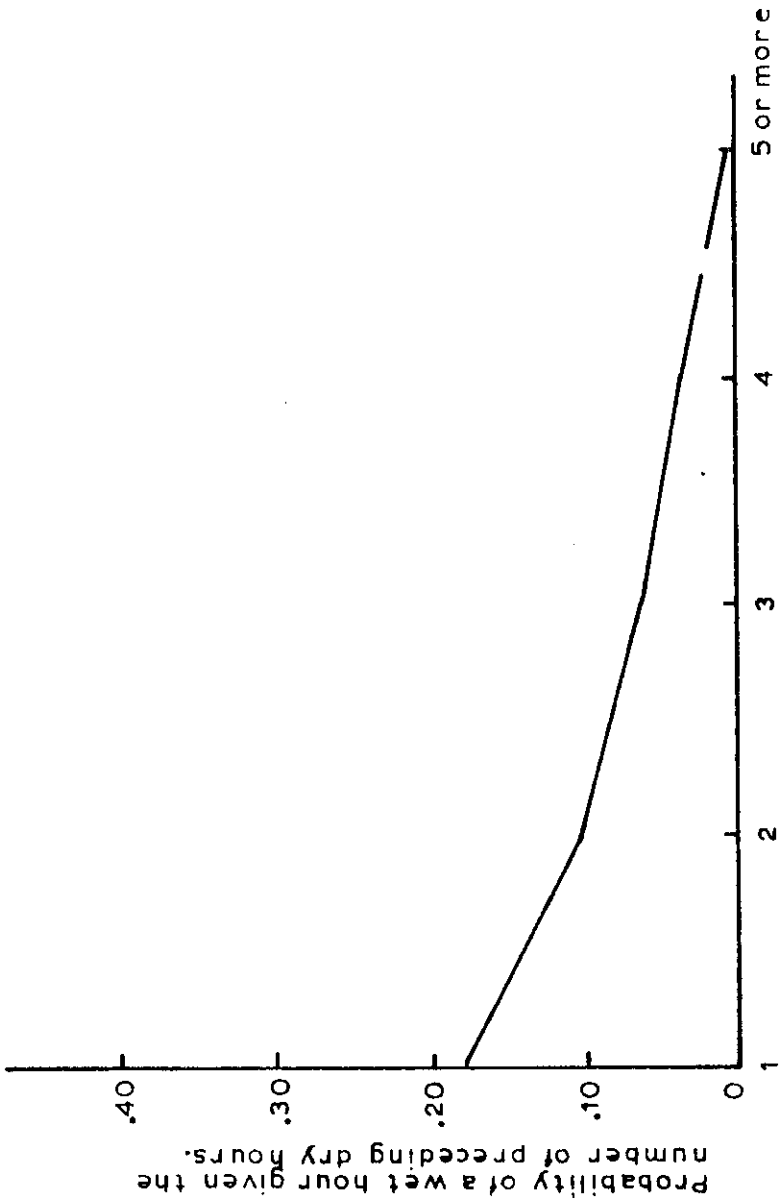

Fig. 10. Transition probabilities following dry periods.

all periods from time (t) through time (t-5) are equal to 1 hr. Time (t-6) ends with the hour immediately preceding time (t-5) and is defined as wet if any precipitation occurs within the 24-hr period immediately preceding time (t-5). Table 5 gives the transitional probabilities for the secondary portion of the Markov chain. D and W denote dry and wet, respectively. The secondary portion is assumed stationary for all time periods. Table 6 illustrates the complete scheme (primary and secondary portions) for the sixth-order Markov chain.

Rainfall-Runoff Simulation

Monte Carlo simulation with the Markov chain is basically simple. Regardless of whether the primary or the secondary portion of the chain is being employed, the fundamental procedure is as follows:

1. Obtain the cumulative probabilities corresponding to the existing rainfall type and state. The final cumulative probability should be unity.
2. A number from zero to unity is drawn from a sequence of random numbers which are uniformly distributed.
3. The state for time (t) is selected to correspond

Table 5. Transitional probabilities for the secondary portion of the Markov chain.

State During Time						State During Time (t)	
t-6	t-5	t-4	t-3	t-2	t-1	D	W
D	D	D	D	D	D	.995	.005
D	D	D	D	W	D	.943	.157
D	D	D	W	D	D	.915	.085
D	D	D	W	W	D	.789	.211
D	D	W	D	D	D	.947	.053
D	D	W	D	W	D	.556	.444
D	D	W	W	D	D	.937	.063
D	D	W	W	W	D	.857	.143
D	W	D	D	D	D	.968	.032
D	W	D	D	W	D	.667	.333
D	W	D	W	D	D	.800	.200
D	W	D	W	W	D	.875	.125
D	W	W	D	D	D	.924	.076
D	W	W	D	W	D	.714	.286
D	W	W	W	D	D	.927	.073
D	W	W	W	W	D	.866	.134
W	D	D	D	D	D	.984	.016
W	D	D	D	W	D	.830	.170
W	D	D	W	D	D	.865	.135
W	D	D	W	W	D	.783	.217
W	D	W	D	D	D	.933	.067
W	D	W	D	W	D	.783	.217
W	D	W	W	D	D	.866	.134
W	D	W	W	W	D	.878	.122
W	W	D	D	D	D	.960	.040
W	W	D	D	W	D	.781	.219
W	W	D	W	D	D	.887	.113
W	W	D	W	W	D	.814	.186
W	W	W	D	D	D	.938	.062
W	W	W	D	W	D	.723	.277
W	W	W	W	D	D	.897	.103
W	W	W	W	W	D	.834	.166

Table 6. Complete scheme for the sixth-order Markov chain.

Time Period Used in Model	Clock Hour	Possible States
Time (t)	Hour (t)	Class 1, 2, ..., 10
Time (t-1)	Hour (t-1)	Class 1, 2, ..., 10
Time (t-2)	Hour (t-2)	Wet - or - Dry
Time (t-3)	Hour (t-3)	Wet - or - Dry
Time (t-4)	Hour (t-4)	Wet - or - Dry
Time (t-5)	Hour (t-5)	Wet - or - Dry
Time (t-6)	Hour (t-6) Hour (t-7) . . . Hour (t-29)	Wet - or - Dry

to the smallest cumulative probability greater than the random number.

Several authors have used autoregressive or Markov-chain models for monthly or yearly streamflow (Thomas and Fiering, 1962; Julian, 1961; Brittan, 1961). However, Pattison's work (1964) represents the first attempt to simulate rainfall by a Markov chain for input to a runoff model. The aim of Pattison's over-all procedure was to produce long records of synthetic streamflow (months or years).

The aim of the present study is to use the Markov-chain model presented above as a forecast tool for an individual storm. Knowing the amount of rainfall that occurred during time (t-1) and the preceding 28 hr period, one can make a probabilistic forecast for the next hour, time (t). Time (t) then becomes time (t-1), time (t-1) becomes time (t-2), etc., and the procedure is iterated. Six-hour precipitation forecasts are used in this study.

Six-hour precipitation forecasts were made for each subarea of the watershed (see Fig. 4). The 29 hr of antecedent rainfall needed for the Markov chain simulation was assumed to be the average rainfall for the subarea, and the rainfall forecast for each subarea is assumed to be the average for the subarea. To test the procedure, forecasts were made for two events in which data could

be obtained from the ARS rain-gage network (see Fig. 1). Once the forecast rainfall for each subarea was determined, the runoff for each subarea was calculated by Eq. 11. After the runoff for each subarea was obtained, the lag time and peak discharge then could be computed from Eqs. 12 and 13, respectively. The computed peak discharge then was deposited in one of one hundred equally-spaced classes. The classes were divided into 100-cfs class intervals and, thus, encompass discharges from 0 to 10,000 cfs. The simulation procedure was repeated for a total of 500 iterations. The forecast procedure would be the same regardless of the source of rainfall information, e.g., radar-estimated rainfall.

A Fortran IV computer program was written for the rainfall-runoff simulation. The computer output consisted of a frequency histogram of hydrograph-peak discharges and corresponding lag times. From the frequency histogram, the peak discharge and lag time occurring with the greatest frequency was determined; this peak discharge then represented the most probable value. Similarly, peak discharges of various frequencies and corresponding probabilities were obtained. A block diagram of the computational scheme for the rainfall-runoff simulation is presented in Fig. 11.

Fig.11. A block diagram of the computational scheme used for rainfall-runoff simulation with the stochastic model.

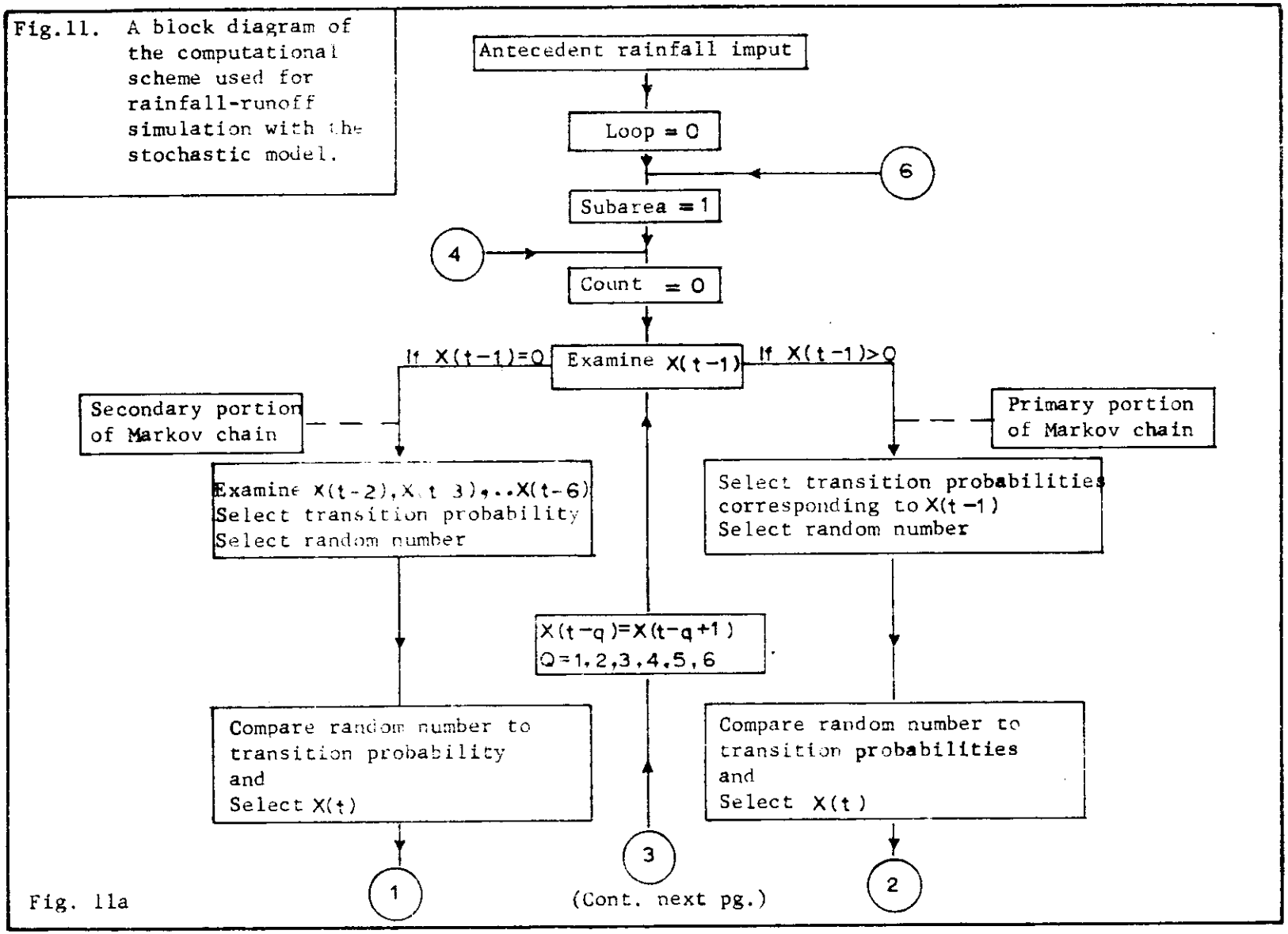

Fig. 11a

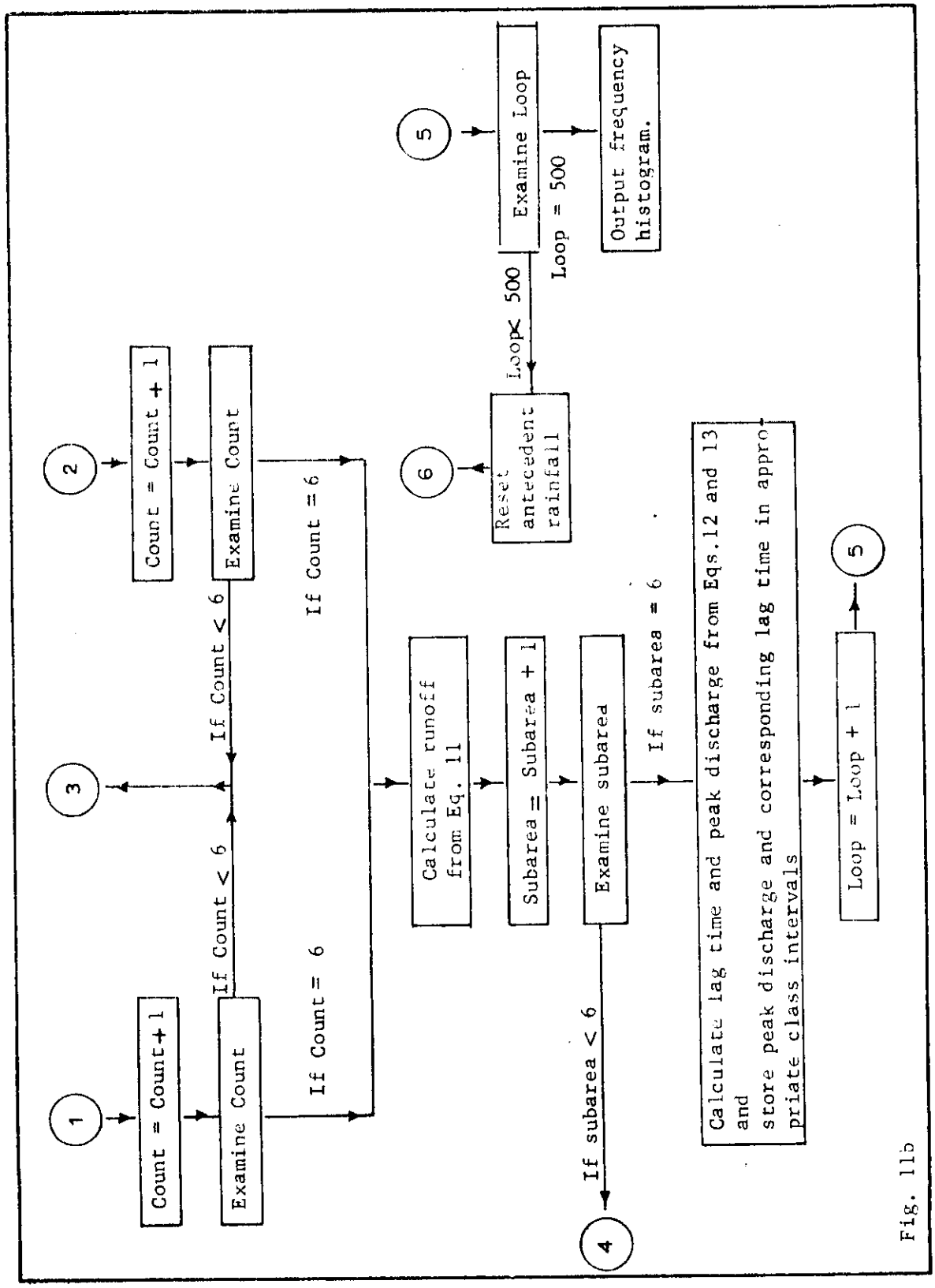
1
Count = Count + 1
Examine Count
If Count < 6
If Count = 6
2
Count = Count + 1
Examine Count
If Count < 6
If Count = 6
3
Calculate runoff from Eq. 11
Subarea = Subarea + 1
Examine subarea
If subarea = 6
If subarea < 6
4
Calculate lag time and peak discharge from Eqs.12 and 13 and
store peak discharge and corresponding lag time in appropriate class intervals
Loop = Loop + 1
5
5
Examine Loop
Loop < 500
Loop = 500
Output frequency histogram.
6
Reset antecedent rainfall

Fig. 11b

C H A P T E R I V

PRESENTATION AND DISCUSSION OF RESULTS

Success of Runoff Predictions

Table 7 summarizes the runoff based on the various rainfall measurements. The predictions may be compared to each other and to the observed runoff, which also is listed in Table 7. The following observations can be made from Table 7.

1. Runoff was forecast from measurements by radar for all four storms.
2. For the four storms the runoff predictions derived from the two ARS rain gages are as good as or better than the predictions derived from radar measurements.
3. Appreciable error was made in the runoff prediction for storm 19 even with measurements taken with the dense ARS rain-gage network.

Based on observation No. 1 it might be concluded that the radar possess potential for use as a hydrologic tool. The prediction of an amount of runoff, even though the prediction may be in error, is better than no prediction. This result indicates that if no rain gages are available, the radar, even under the worst circumstances, will yield answers that are better than no answers.

Table 7. Average precipitation and runoff derived from various rainfall measurements compared to each other and to observed runoff.

Storm No.	Date	ARS Rain-Gage Network		NSSL Radar		Two Rain Gages (ARS Gages 137 and 151)		Observed	
		P(in)	E(in)	P(in)	E(in)	P(in)	E(in)	P(in)	E(in)
19	5/9/64	2.10	0.166	0.85	0.075	1.83	0.137	----	0.385
20	5/9/65	0.49	0.025	0.28	0.017	0.61	0.027	----	0.024
21	5/30/64	0.26	0.041	0.60	0.080	0.14	0.022	----	0.031
22	5/10/64	0.59	0.079	0.47	0.067	0.86	0.106	----	0.086

The two ARS rain gages constitute a gage density which is superior to that normally encountered for hydrologic work. In addition, the location of the two gages on opposite ends of the watershed constitute an optimum gage arrangement. While the quantitative prediction of precipitation and runoff derived from measurements taken with the two ARS gages appear somewhat superior to those based on radar measurements, the radar actually proved superior for depicting the spatial distribution of the rainfall for storm 20.

Observation No. 3 stresses the importance of obtaining a satisfactory equation for runoff prediction, Eq. 11. The inadequacies accompanying the derivation of Eq. 11 were discussed in Chapter II. Great effort should be placed on the development of the equation for prediction of runoff for operational forecasting. The equation, hopefully, should lead to forecasts of accurate amounts of runoff for a storm of any magnitude.

Feasibility of Radar, Rain-Gage Combination

ARS gage 147 was used in combination with measurements made by radar for storm 19, and estimates of lag time and peak discharge were made (see Table 8). For storm 19 a considerable improvement in prediction was obtained by the use of the radar, rain-gage combination

Table 8. Lag times and peak discharges derived from various rainfall measurements compared to the observed values.

Storm No.	Date	ARS Rain-Gage Network		NSSL Radar		NSSL Radar Adjusted by ARS Rain-Gage 147		Two Rain Gages (ARS Gages 137 and 151)		Observed	
		Lg (hr)	Q_p (cfs)	Lg (hr)	Q_p (cfs)	Lg (hr)	Q_p (cfs)	Lg (hr)	Q_p (cfs)	Lg (hr)	Q_p (cfs)
19	5/9/64	6.43	3250	6.73	1495	6.67	2540	6.98	2570	6.85	9190
20	5/9/65	7.30	500	6.55	367	----------		8.10	503	6.75	540

over estimates made from radar measurements alone. As illustrated in Chapter II, storm 19 is evenly distributed over the watershed. For this storm the radar consistently underestimated the rainfall over the entire watershed. The hourly correction factors applied to the "radar-measured" rainfall increased the rainfall quantities to amounts commensurate with those obtained with the ARS rain-gage network. It appears that the improvement in rainfall measurement acquired through the radar, rain-gage combination results largely from the fact that storm 19 was evenly distributed over the basin. Therefore, as a further test, the rainfall amounts for storm 20, which was unevenly distributed over the watershed, were considered for estimation by the radar, rain-gage combination. However, the obvious difficulty linked with this approach occurred with storm 20; i.e., essentially no rainfall was observed at ARS rain-gage 147 (see Fig. 8). Thus, adjustment of the "radar-measured" rainfall by rain-gage 147 was not feasible. A desirable, but impossible arrangement would be the use of a mobile rain gage for calibration of the weather radar.

Comparison of Lag-Time Estimates

Table 8 lists the estimates of lag time as derived from various rainfall measurements. Also, the observed

lag times are presented for comparison. The estimates of lag time, based on measurements performed with radar, are excellent for both storms 19 and 20; the differences between the predicted and observed lag times were less than 3 per cent in both instances. The estimate of the lag time for storm 19, derived from rainfall measurements taken with the two ARS rain gages, also is very good. As pointed out above, storm 19 is evenly distributed over the watershed. Therefore, a lag-time estimate based on only two rain gages gave satisfactory results. However, appreciable error (20 per cent) occurred in the estimate for lag time, derived from the two rain gages, for storm 20. This sizable error emphasizes the superiority of the radar over a sparse rain-gage network for depicting the spatial distribution of rainfall when a storm is unevenly distributed over the basin.

Comparison of Hydrograph Predictions

Hydrographs were synthesized with the Pearson type III function for storms 19 and 20. Fig. 12 presents a comparison of the hydrographs, computed from the various rainfall inputs and the Pearson function, to the observed hydrograph for storm 19.

As mentioned previously, all estimates of runoff for storm 19 are considerably lower than that which was

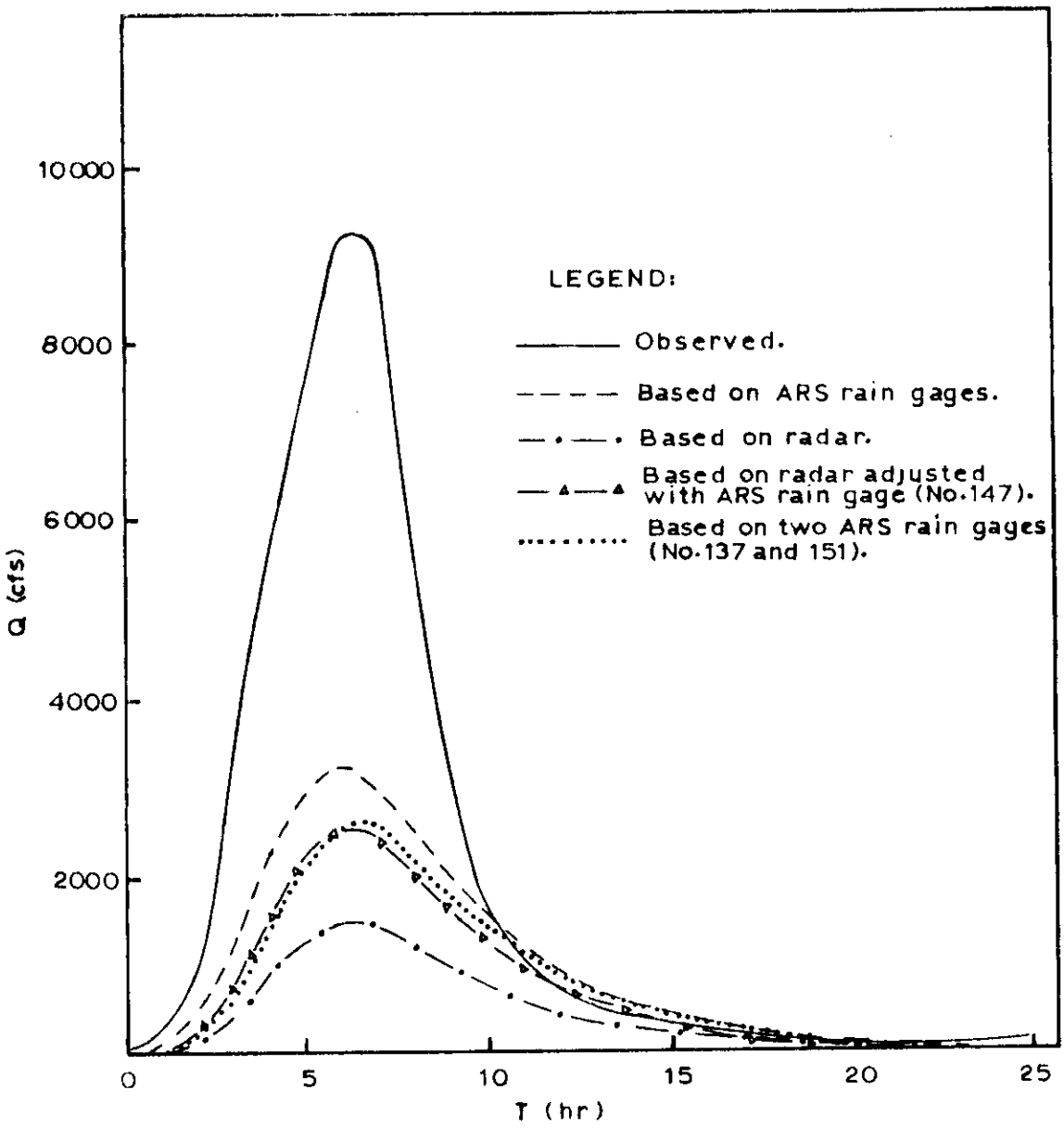

Fig. 12. Comparison of synthesized hydrographs, computed using various rainfall inputs and the Pearson function, to the observed hydrograph for the storm of May 9, 1964.

observed. Since the peak discharge is directly proportional to the amount of runoff (see Eq. 13) the hydrograph peaks are all considerably underestimated. However, the hydrograph computed from rainfall measurements obtained with the radar, rain-gage combination compares favorably to the hydrograph based on the ARS rain-gage network.

The hydrographs synthesized for storm 20 with the Pearson function are presented in Fig. 13. While the peak discharge for the "radar-predicted" hydrograph was substantially lower than the peak discharge for the observed hydrograph, the estimated time of arrival for the maximum discharge was quite accurate. Examination of Fig. 13 reveals that the observed hydrograph for storm 20 is complex (two peaks). Fig. 14 is a comparison of the hydrographs synthesized from the linear-routing model developed in Chapter II and various rainfall measurements. It was hoped that the routing model would satisfactorily reproduce the two peaks observed for storm 20, but it failed to do so. The two peaks were not the result of two separate bursts of rainfall but, rather, are a result of an uneven distribution of rainfall excess which occurred over the basin. The tributary arrangement in the vicinity of the maximum rainfall (see Fig. 8) gives a large gradient of travel time (see Fig. 4). This

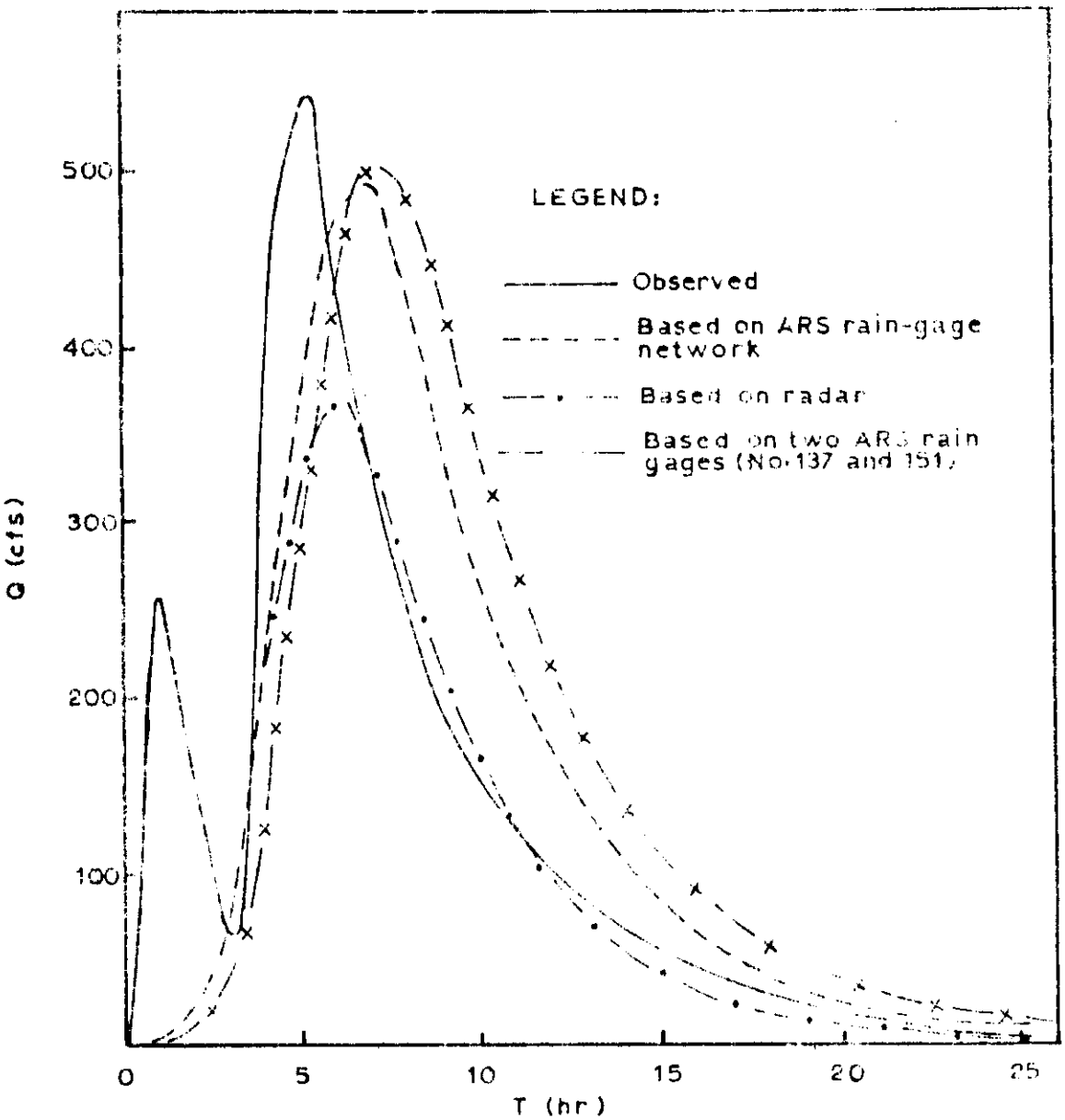

Fig. 13. Comparison of synthesized hydrographs, computed using various rainfall inputs and the Pearson function, to the observed hydrograph for the storm of May 9, 1965.

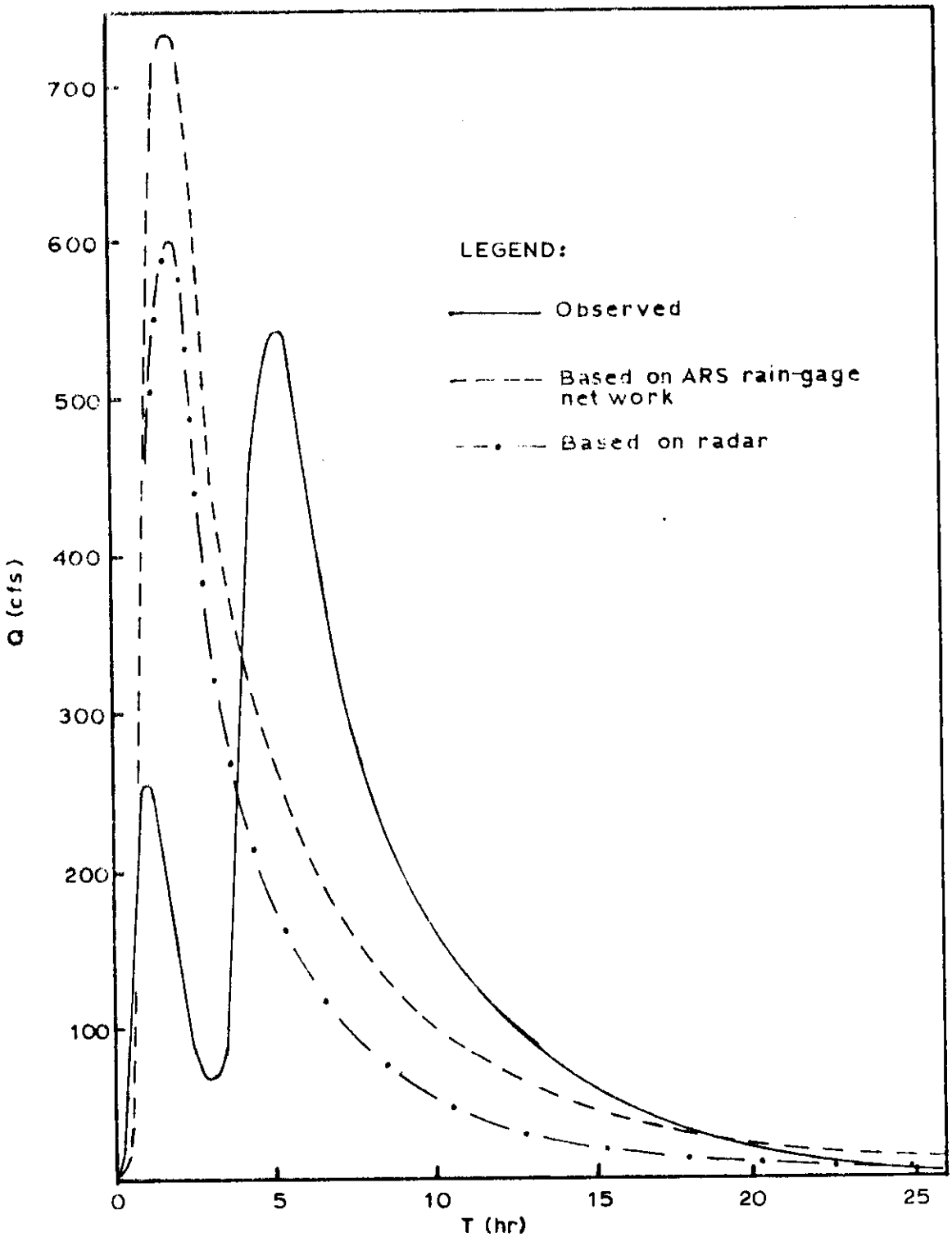

Fig. 14. Comparison of synthesized hydrographs, computed using various rainfall inputs and the routing model, to the observed hydrograph for the storm of May 9,1965.

fact, coupled with the large gradients of precipitation in this same locality, is believed to be responsible for the occurrence of the two peaks. However, for the combination of subareas selected (see Fig. 4), the routing procedure was unable to detect the two peaks. In fact, it actually predicted the hydrograph peaks several hours earlier than the Pearson function.

A possible improvement in the routing procedure might be attained by considering a series of linear storages between each subarea and the outlet. That is, the total storage delay time for each subarea could be segmented into several storage coefficients and multiple routing performed from each subarea to the outlet. Laurenson (Sect. 5.5.1, 1962) has investigated a linear routing model which assumes a series of concentrated storages between each subarea and the outlet. Laurenson concluded that a non-linear routing model was more appropriate for his basin. However, since the storage equation for the Little Washita is assumed to be linear, a procedure similar to the one investigated by Laurenson for linear routing might represent an improvement over the routing model adopted for this study.

To illustrate the importance of an accurate prediction of runoff for hydrograph synthesis, the hydrograph for storm 19 was synthesized from the Pearson function

with the runoff set equal to the observed amount. While there is still some error in the prediction of the peak discharge from Eq. 13, an improvement of over 100 per cent is observed (see Fig. 15). This illustration once again stresses the importance that should be placed in the development of the runoff-prediction equation (Eq. 11 in this study).

Success of Stochastic Model

Figure 16 is a frequency histogram of the hydrograph-peak discharges as derived from the stochastic model for storm 19. The numbers appearing on the bars are the average lag times for the class intervals. The most probable interval of the peak discharge is the one occurring with the greatest frequency (2400-2700 cfs). While the most probable value for the peak discharge (say 2550 cfs) is substantially lower than the observed peak discharge (9190 cfs), it compares quite favorably with the peak discharge derived from rainfall measurements made with the ARS rain-gage network (3250 cfs). In fact, the frequency histogram indicates that a peak discharge of 3250 cfs is possible (probability of about 0.10).

Figs. 17, 18, and 19 are the frequency histograms of hydrograph-peak discharges for storm 20. The observed

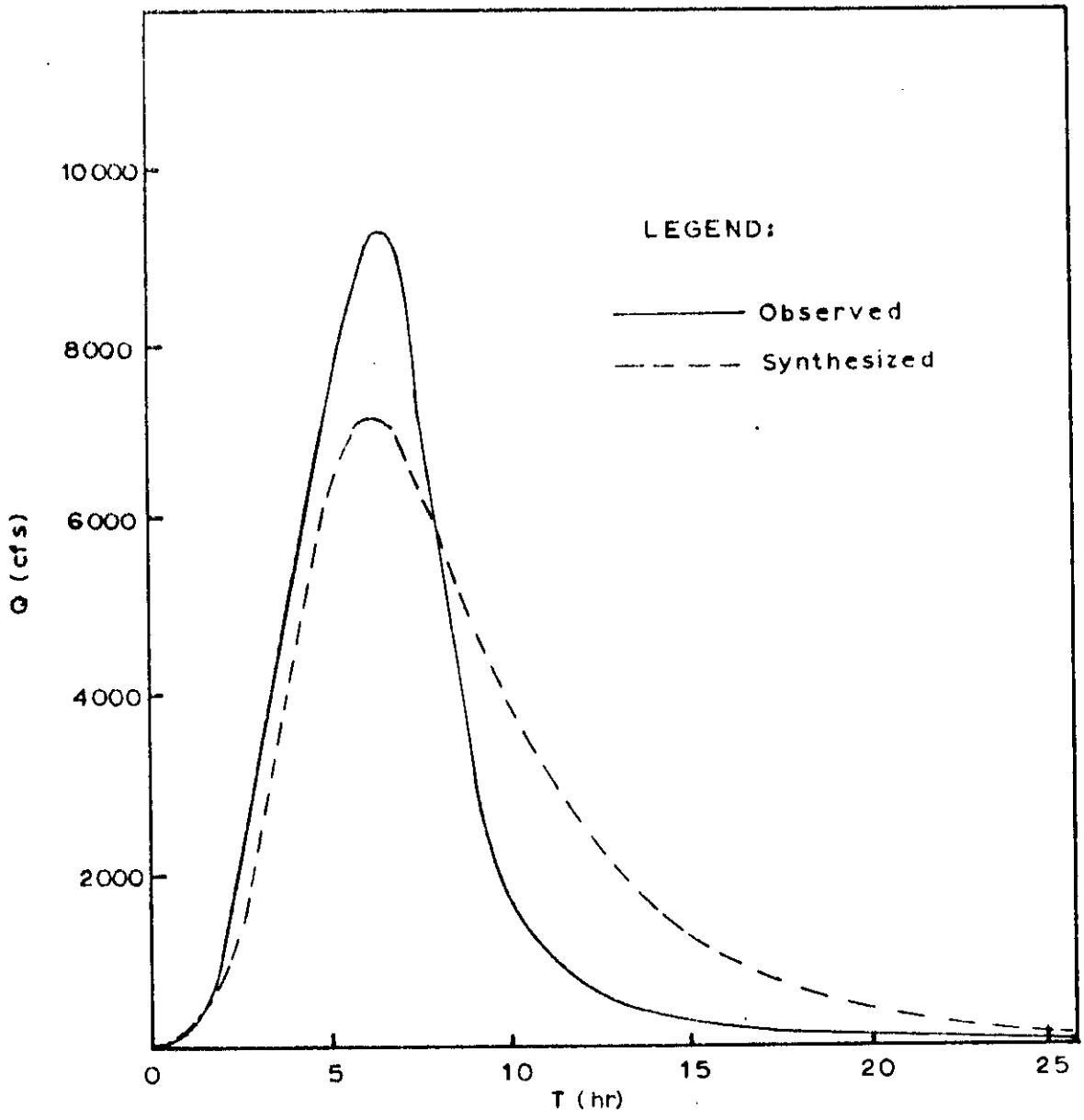

Fig. 15. Comparison of synthesized hydrograph, computed using observed runoff and lag time with the Pearson function, to the observed hydrograph for the storm of May 9, 1964.

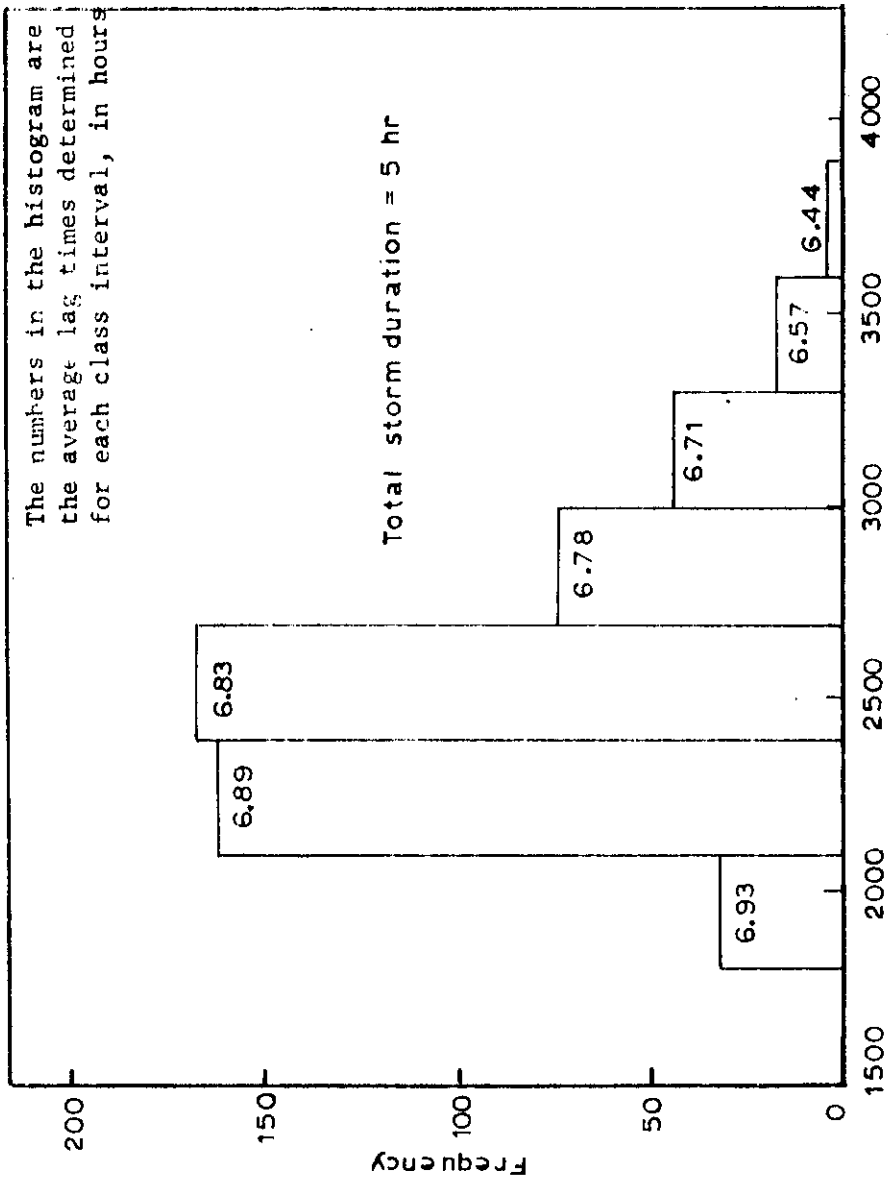

Fig. 16.- Frequency histogram of hydrograph-peak discharges, as derived from the stochastic model (storm of 9 May 1964, 1st hour of rainfall given).

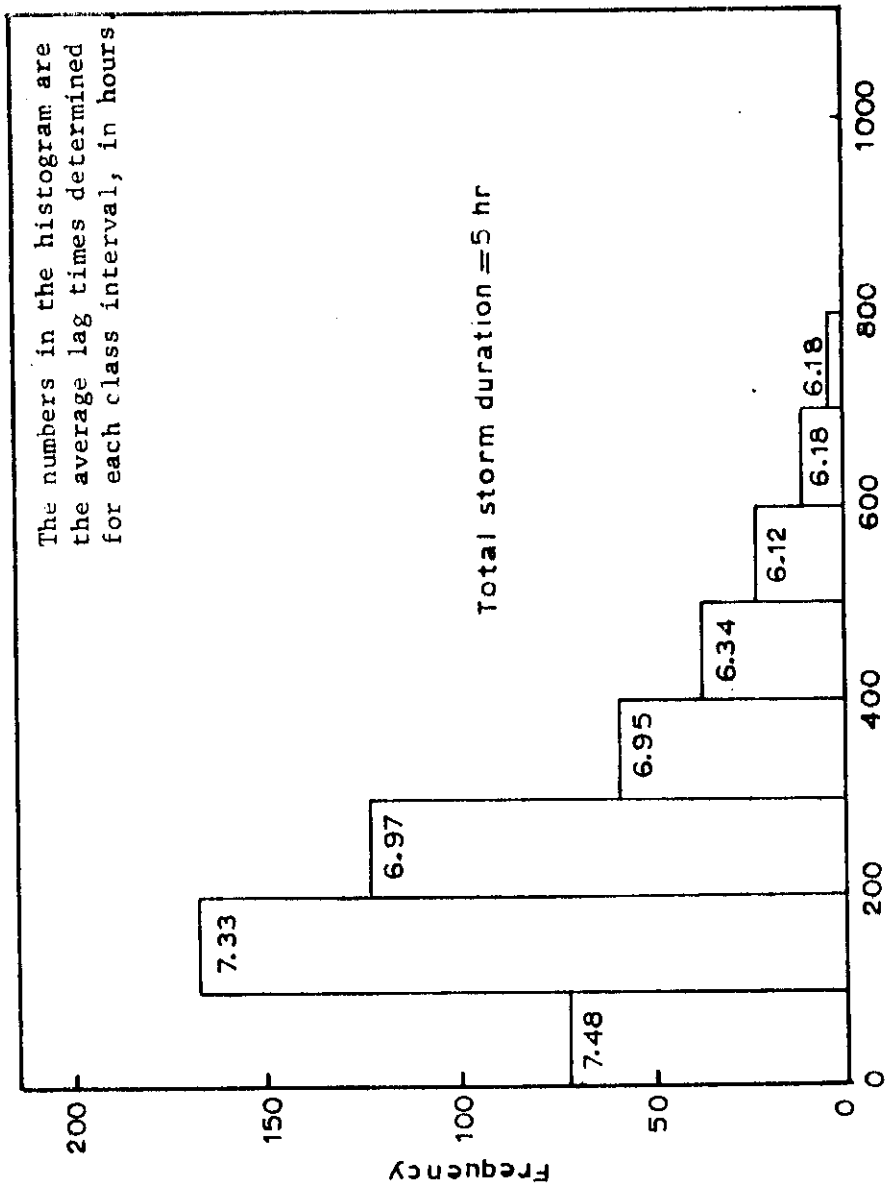

Fig. 17. Frequency histogram of hydrograph-peak discharges, as derived from the stochastic model (storm of 9 May 1965, 1st hour of rainfall given).

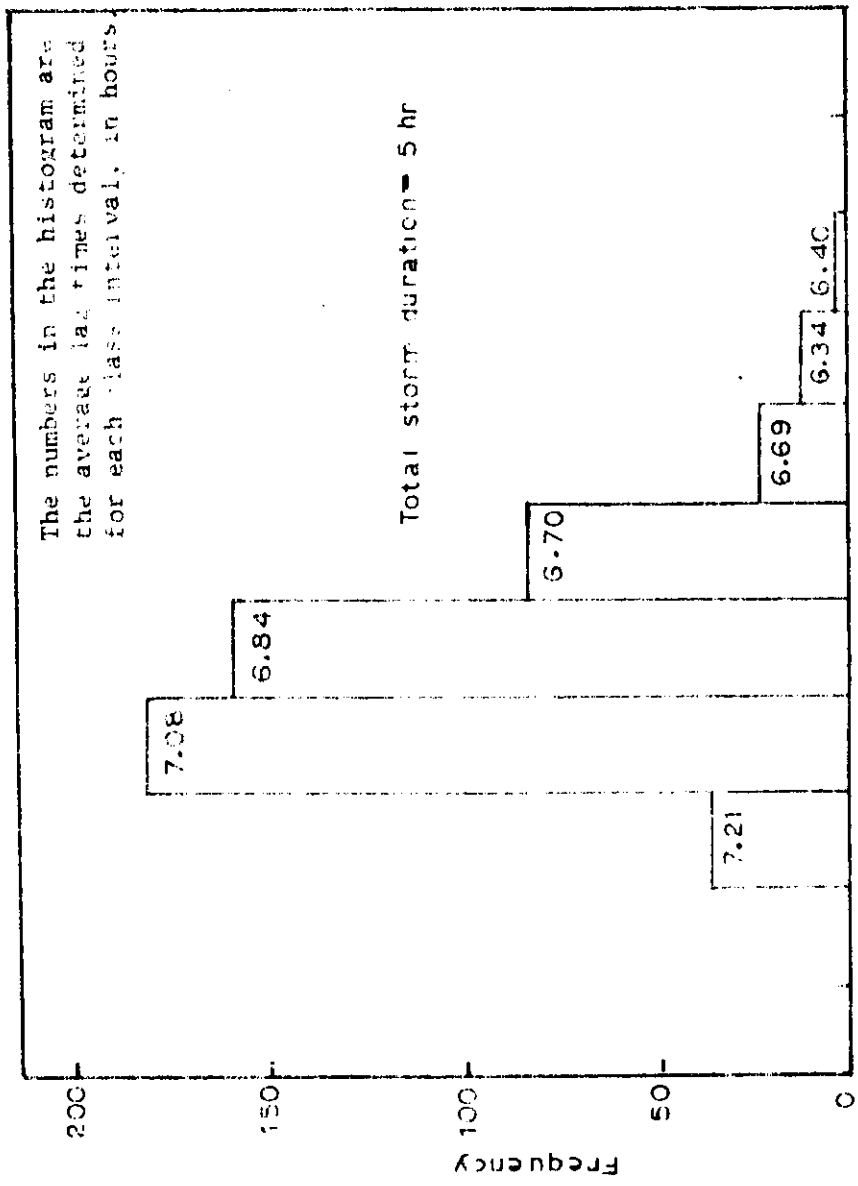

Fig. 15. Frequency histogram of hydrograph-peak discharges, as derived from the stochastic model (storm of 9 May 1965, 1st two hours of rainfall given).

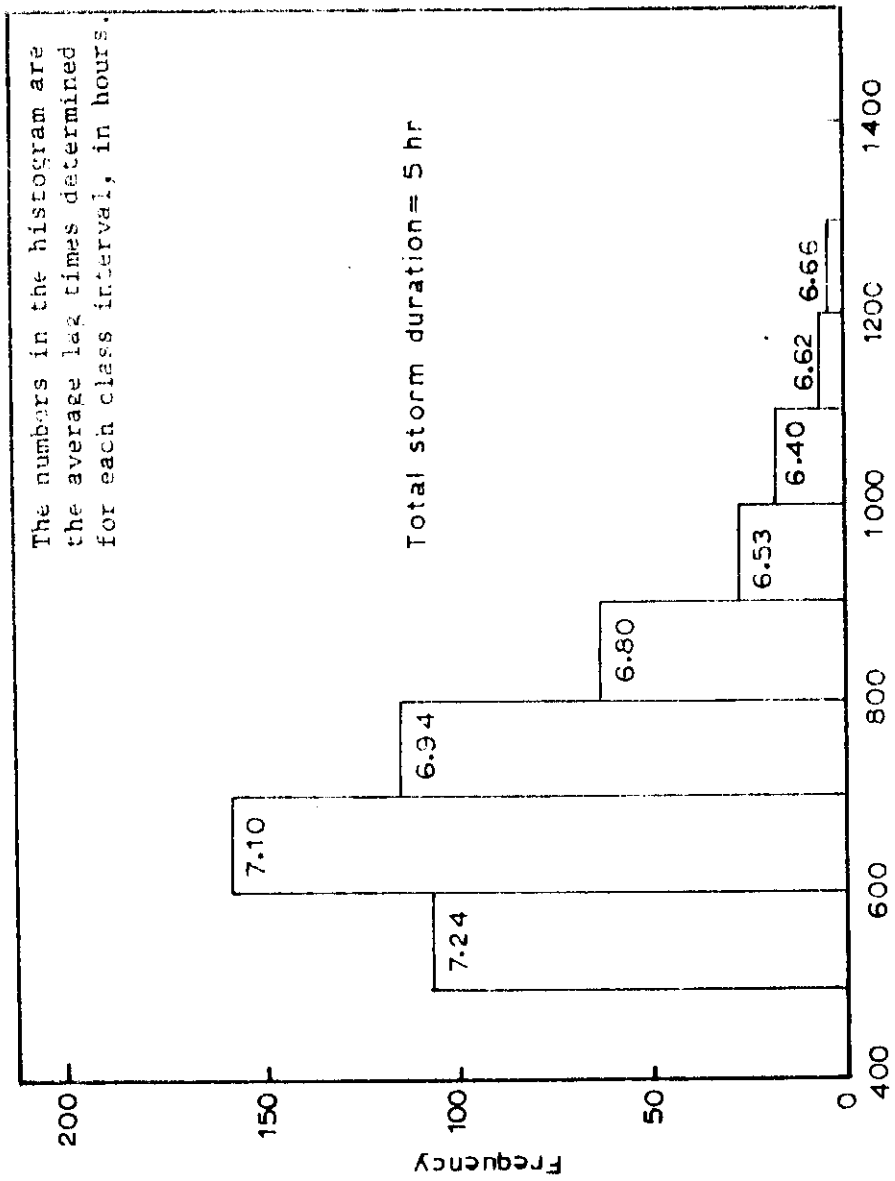

Fig. 19. Frequency histogram of hydrograph-peak discharges, as derived from the stochastic model (storm of 9 May 1965, 1st three hours of rainfall given).

peak discharge for storm 20 was 540 cfs. Examination of Figs. 17, 18, and 19 shows that an improvement in the prediction of the peak discharge occurs with the addition of successive hours of "known" rainfall. The occurrence of a peak discharge of 540 cfs is possible from all three histograms. The most surprising of the three cases is the one represented by Fig. 17. The rainfall experienced during the first hour of storm 20 was very slight (less than 0.05 in. for every subarea). Thus, the model might be expected to predict negligible runoff; however, a relatively high probability (0.25) of getting a peak discharge from 300 to 400 cfs is indicated.

The results from the stochastic model are promising. A stochastic model, such as the one developed in this study, could be coupled with radar measurements to obtain a probabilistic forecast of streamflow shortly after rainfall commencement.

CHAPTER V

CONCLUSIONS AND RECOMMENDATIONS

Conclusions

It is realized that some of the procedures proposed in this study (particularly the stochastic technique for the simulation of rainfall-runoff) will require further testing with additional storms before their real value can be assessed. Nevertheless, the potential usefulness of the proposed procedures has been demonstrated. The following conclusions may be inferred from this study:

1. Quantitative estimates of runoff can be made from measurements taken with weather radar. In the derivation of procedures for operational forecasting, great effort should be placed in the development of the runoff-prediction equation (Eq. 11 in this study). If the amounts of runoff and the spatial distribution of the rainfall excess are estimated accurately, satisfactory streamflow forecasts can be made.
2. Accurate estimates of lag time can be made from radar observations. The radar is superior to a sparse rain-gage network (1 gage/110 mi^2) for depicting the areal distribution of rainfall;

this is especially true for storms which are unevenly distributed over the watershed.

3. A radar, rain-gage combination represents a potentially useful arrangement for rainfall measurements if a storm produces appreciable depths of precipitation over the entire basin. Adjustment of radar-derived measurements to conform to rain-gage observations may present difficulties if the precipitation is of a showery type.
4. Hydrograph synthesis with the Pearson type III function constitutes a valuable tool for streamflow forecasting. Since this method of hydrograph synthesis is adaptable to the digital computer, the "time factor" for analysis is very short. Although some of the modern techniques for runoff routing might prove profitable for certain watersheds, the technique for hydrograph synthesis with the Pearson type III function should constitute a valid approach for most basins since temporal and spatial variations in rainfall are considered in the scheme.
5. A stochastic model, such as the one developed in this study, offers great possibilities as a probabilistic forecasting tool. The sixth-order

Markov chain appears to reproduce adequately the rainfall process for Ninnekah, Oklahoma. A stochastic model coupled with radar measurements will make possible a probabilistic forecast of streamflow shortly after rainfall commencement.

Recommendations

Some areas for further research are suggested by this study.

1. The techniques developed in this study should be tested on additional storms. The storms selected should display variable characteristics (e.g., storms with different temporal and spatial distributions, durations, and total amounts of rainfall should be chosen). In addition, storms associated with all six synoptic types named in Chapter III should be selected for further examination of the stochastic model.
2. Similar relationships should be derived for another watershed. A watershed which has experienced a sizable number of large runoff events (greater than 50 cfs/mi^2) would be desirable.

3. Before operational streamflow forecasting can be made practical, rapid methods for data collection, processing, and communication must be developed. The staff at NSSL are making major progress in these areas and hope to have a "real-time" system in the near future. In order to obtain a better runoff forecast, additional refinement in the radar hardware should be considered--in particular, smaller gain-step intervals would be desirable.
4. Since calibration of the radar by one or more rain gages may not be feasible in many instances, techniques for the selection of an appropriate Z-R relationship for a particular storm must be found. As mentioned in Chapter II, utilization of statistics derived from radar patterns should prove useful.
5. Stochastic hydrology is still in its infancy; thus, many hydrologic problems which may be handled by stochastic procedures require further research. Recommendations No. 1 and 2 above should be considered in connection with the stochastic model developed in this study. In addition, the following two recommendations are made:

a. Additional research is needed to assess the dependability of the procedure used in this study for synthesis of rainfall on an areal basis. A stochastic model which considers point rainfall input and which forecasts point rainfall actually may be desirable. If a stochastic model is used in conjunction with weather radar, the grids which constitute the radar network could be assumed as point sources. Development of restraints which force compatible results (prevent improbable gradients) among grids might be incorporated into the model.

b. The possibility of shortening the time, to less than 1 hr, needed after storm commencement before a reliable forecast can be made should be investigated. For a given "synoptic type" the rainfall which occurs in the first minutes of the storm (say 15 min) frequently will give an indication of the amount to fall during the remainder of the hour.

APPENDIX A

Least-Squares Technique for Fitting Hydrograph Data

A procedure was developed for fitting the Pearson type III function to seven points on the surface runoff hydrograph. The procedure is the same for any function which leads to non-linear normal equations and for varying quantities of data. A Fortran IV program was written for the procedure; the flow diagram is presented at the end of the appendix (Fig. 21). It is assumed also that the reader is familiar with the conventional least-squares procedure.

Since the hydrograph must contain an area equivalent to the volume of runoff, the least-squares procedure must be designed accordingly. If Pearson's function defines the unit hydrograph, the area under the curve can be evaluated from the integral

$$\text{AREA} = \int_{o}^{\infty} Q\,dt = \int_{o}^{\infty} Q_p (T/P_r)^a \exp[-(T-P_r)/c]\,dT \ , \quad (26)$$

or

$$\text{AREA} = \frac{Q_p \exp(P_r/c)}{P_r^a} \int_{o}^{\infty} T^a \exp(-T/c)\,dT \ . \quad (27)$$

Eq. 27, when integrated, becomes

$$\text{AREA} = \frac{Q_p \exp(P_r/c) c^{(a+1)}}{P_r^a} [\Gamma(a+1)] \tag{28}$$

where Γ denotes the Gamma function. For large positive values of a, $\Gamma(a)$ may be approximated by a truncated form of the Stirling formula,

$$\Gamma(a) = a^a \exp(-a) \sqrt{(\frac{2\pi}{a})} (1 + \frac{1}{12a} + \frac{1}{288a^2}) , \tag{29}$$

Since $\Gamma(a) = a\Gamma(a)$ for a greater than zero, Eq. 28 becomes

$$\text{AREA} = \frac{Q_p \exp(P_r/c) (ca)^{(a+1)}}{P_r^a e^a} \sqrt{(\frac{2\pi}{a})} (1 + \frac{1}{12a} + \frac{1}{288a^2}) K , \tag{30}$$

where K is a conversion factor which relates AREA in inches.

Examination of Eq. 30 reveals that neither c nor a can be written explicitly. For a specified AREA, an iterative solution must be adopted to determine c or a. Newton's method for the numerical solution of equations is appropriate when solving for c from Eq. 30 (see Stanton, 1961, p. 84). Newton's procedure may be described by

$$c_n = c_o - f(c_o)/f'(c_o) \quad , \tag{31}$$

where c_n is the new estimate and c_o the old estimate. The prime indicates the first derivative. The process is repeated until a negligibly small difference occurs between c_n and c_o. Because the Newton process is a second-order process (involves the first derivative), the root is approached with great rapidity.

In order to apply Eq. 31, Eq. 30 can be written in the following form:

$$f(c) = 0 = c - P_r/\{\ln(AREA) - \ln[Q_p(P_r e)^{-a}(ca)^{(a+1)}\sqrt{(\tfrac{2\pi}{a})}(1 + \tfrac{1}{12a} + \tfrac{1}{288a^2})K]\} \tag{32}$$

and

$$f'(c) = 1 - (a+1)P_r/\{c[\ln(AREA) - \ln[Q_p(P_r e)^{-a}(ca)^{(a+1)}\sqrt{(\tfrac{2\pi}{a})}(1 + \tfrac{1}{12a} + \tfrac{1}{288a^2})K]]^2\} \; . \tag{33}$$

Equation 31 was programmed, for solution in Fortran IV language, as a subroutine. The value of c, obtained from the solution of Eq. 31, ensures a runoff volume equivalent to AREA for a preset value of A.

The standard procedure for using the method of

least squares, in which non-linear normal equations arise, depends upon a reduction of the residuals to a linear form by a first-order, Taylor series approximation, which is taken about an initial or trial solution for the parameters (see Levenberg, 1944).

The approximation to Eq. 17 resulting from a first-order, Taylor series expansion around a trial value for the parameter, a, is given by

$$Q = (Q)_{a_o} + \left(\frac{\partial Q}{\partial a}\right)_{a_o}(a - a_o) \quad , \tag{34}$$

where $(\ )_{a_o}$ indicates that the quantity in parenthesis is evaluated with the parameter set equal to the trial parameter, a_o. Terms of a higher order have been ignored.

Let $\beta = a - a_o$

and denote $Q'_a = \frac{\partial Q}{\partial a}$.

Further simplification can be obtained by letting

$$(Q)_{a_o} = Q_o$$

and $$(Q'_a)_{a_o} = Q'_{ao} \ .$$

Eq. 34 now can be written in a simplified form as

$$Q = Q_o + Q'_{ao}\beta \ . \qquad (35)$$

Thus, Eq. 17 can be approximated, for a particular c, by a linear combination in Q_o and Q'_{ao}. The problem is now one of minimizing

$$s = \sum_{i=1}^{7} (Q_{7i} - Q_i)^2$$

or

$$s = \sum_{i=1}^{7} (Q_{7i} - Q_{oi} - Q'_{aoi}\beta)^2 \ , \qquad (36)$$

where the Q_7 points are computed from Eqs. 12, 13, 14, 15, and 16; a positioning of the hydrograph widths at 75 per cent, 50 per cent, and 0 per cent flow has been described in Chapter II. The summation indices will not be carried beyond Eq. 36; however, all indicated terms and subsequent products of these terms must be summed with i ranging from one to seven.

From the calculus, it can be shown that s will be a minimum when the partial derivative of s with respect to β is zero. The resulting equation is

$$s'_\beta = \Sigma(Q_7 - Q_o - Q'_{ao}d)(-Q'_{ao}) = 0 \ . \qquad (37)$$

Eq. 37 can be rearranged to give

$$\beta = \frac{\Sigma(Q_7 - Q_o)Q'_{ao}}{\Sigma(Q'_{ao})^2} \quad . \tag{38}$$

The calculations necessary for the solution of Eq. 38 were programmed as a subroutine separate from the subrouting for obtaining c described above.

The over-all procedure is as follows:

1. A subroutine was developed utilizing Eq. 31 to obtain c for a preset value of a.
2. Next a subroutine was prepared which solved Eq. 38 for β.
3. As pointed out by Hartley (1961), the magnitude of the correction, which is added to the existing trial value for a to obtain the next trial value, is proportional to β. Also, the sign of the correction will be given by the sign of β. This can be expressed mathematically as

$$a^2 = a^1 + v\beta \quad , \tag{39}$$

where the superscripts indicate the trial number and v assumes a value from zero to one. Levenberg (1944) pointed out that when v is equal to one, the process frequently will diverge because of over-correction. Therefore, a suggestion proposed by Hartley (1961) was

adopted for selecting v. Hartley's procedure consists of solving for the error sum of squares (Eq. 36) resulting from the selection of three different v's (initially 0, 0.5, 1). Next a parabola is fit to these values, and the v which results in a minimum error is selected. However, if the minimum error obtained in this manner is not smaller than that occurring when v equals zero, a segment of half-length must be used, etc.

4. The over-all process is repeated until there is no significant change in the parameters (a and c).

Obtaining observed volume of runoff for the hydrograph. If an AREA equal to the runoff volume is utilized in Eq. 31, a considerable reduction is observed in the "goodness of fit" from that resulting from use of a smaller AREA. In addition, the tail of the hydrograph is over-dampened by the Pearson type III function. Therefore, AREA in Eq. 31 was initially set equal to 0.9 of the runoff and the generally accepted practice of adjusting the recession portion of the hydrograph to give the needed runoff volume was adopted. Adjustment begins at the time when the discharge equals 50 per cent of peak discharge on the recession side. The manner in which

the adjustment occurs is depicted by Fig. 20. The computer program was written so that if the standard error exeeded 10 per cent of the peak discharge for AREA equal to 0.9 of the runoff, AREA was reduced until the standard error was less than 10 per cent of the peak discharge, or until AREA was 0.84 of the runoff. AREA was never reduced below 0.84 of the runoff volume.

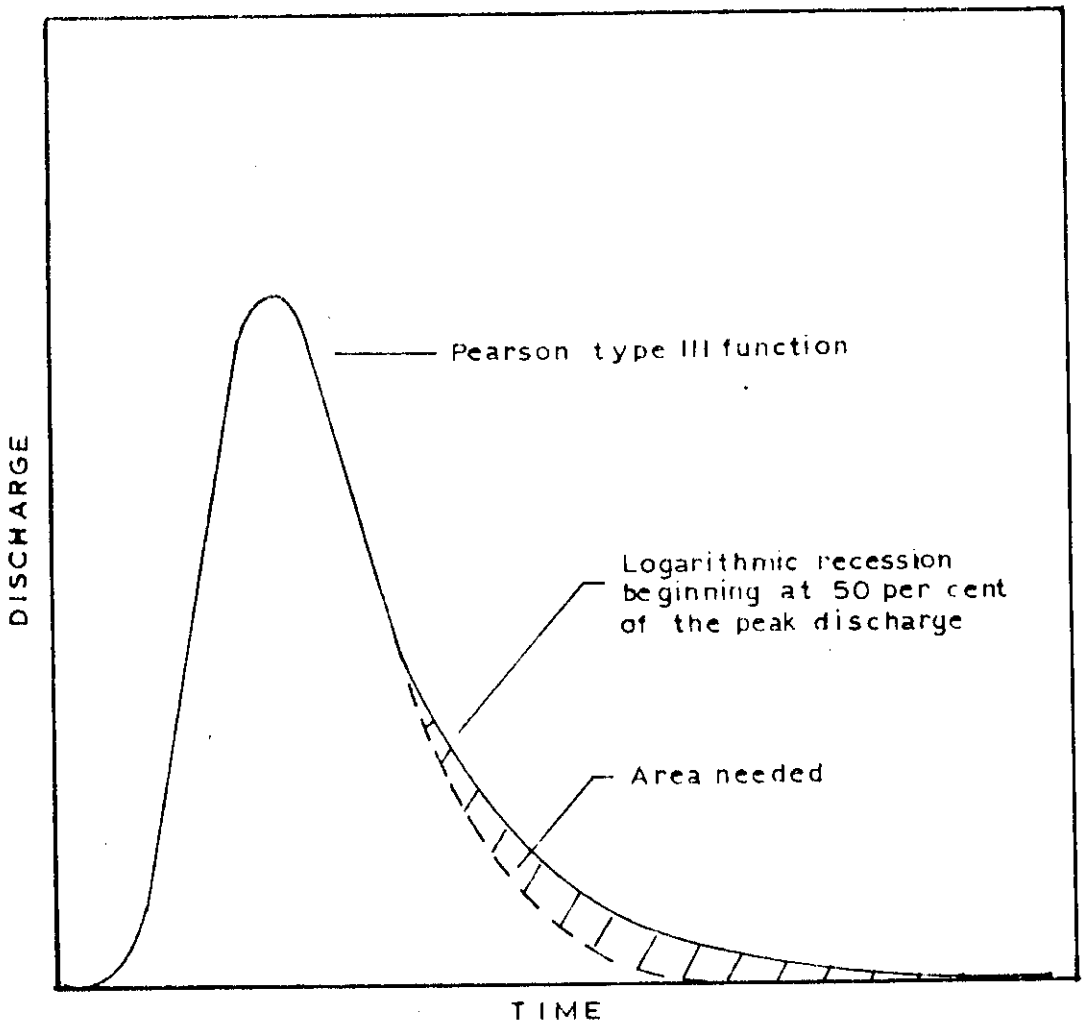

Fig. 20. Pictorial representation of the area added to the hydrograph recession in order to ensure that the total area underneath the hydrograph equals the volume of runoff.

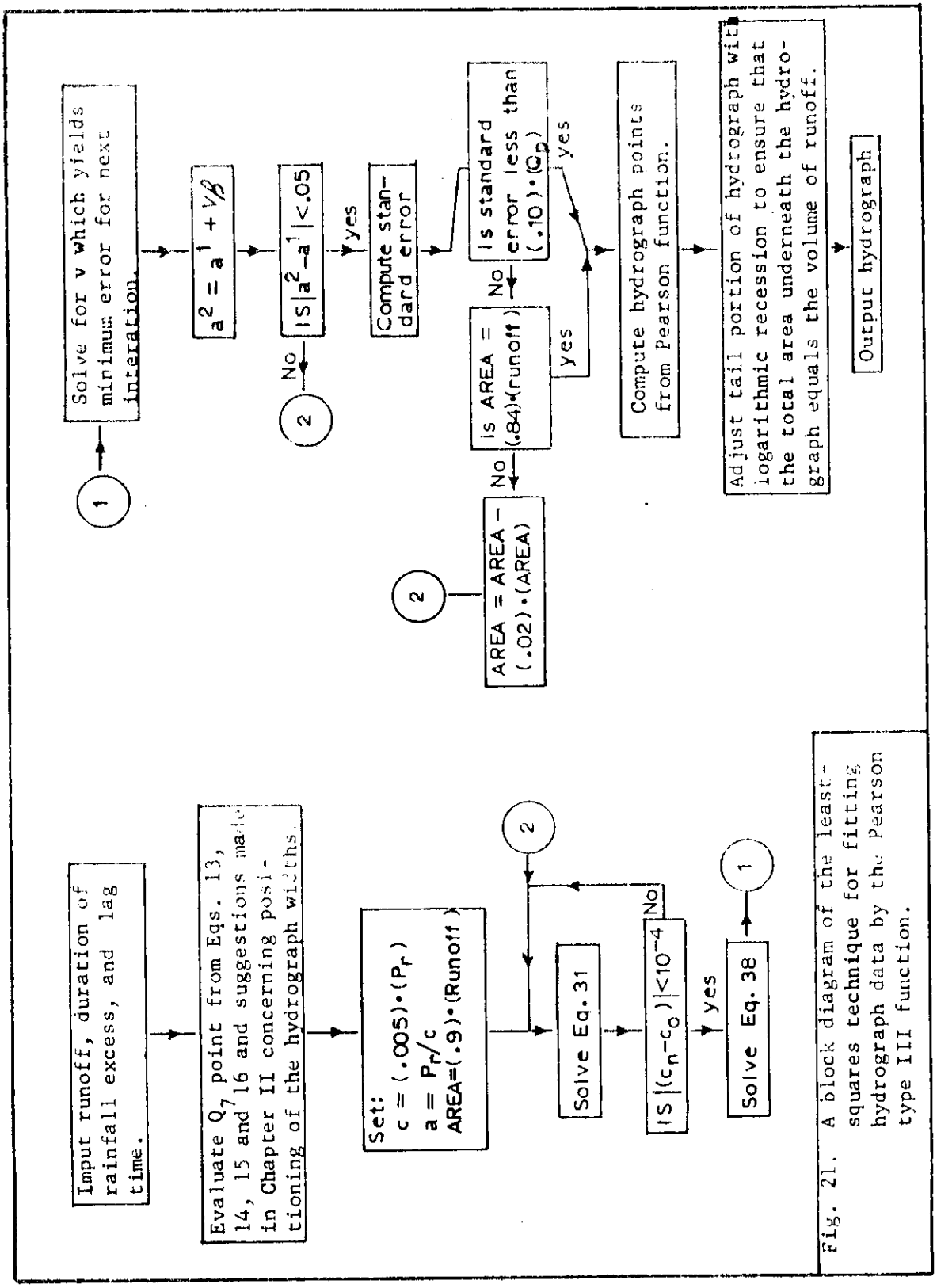

Fig. 21. A block diagram of the least-squares technique for fitting hydrograph data by the Pearson type III function.

APPENDIX B

Analysis of Variance Tables

Table 9. ANOVA for Eq. 11.

Source of Variation	Degrees of Freedom	Sum of Squares	Mean Square	F-Ratio
TOTAL	17	4.678	-----	
Regression	2	3.528	1.764	22.99**
Due to $\overline{R}$	1	1.041	1.041	13.57**
Due to API	1	1.654	1.654	21.56**
Residual	15	1.150	0.0767	

$\pm$ Two Standard Errors = $\begin{matrix} 3.572E \\ 0.279E \end{matrix}$

Table 10. ANOVA for Eq. 13.

Source of Variation	Degrees of Freedom	Sum of Squares	Mean Square	F-Ratio
TOTAL	17	2.223	------	
Regression	2	2.030	1.015	78.68**
Due to E	1	1.555	1.555	120.54**
Due to Lg	1	0.320	0.320	24.81**
Residual	15	0.193	0.0129	

$\pm$ Two Standard Errors = $\begin{matrix} 1.69Q_p \\ 0.59Q_p \end{matrix}$

**Significant at the 1 per cent level.

Table 11. ANOVA for Eq. 14.

Source of Variation	Degrees of Freedom	Sum of Squares	Mean Square	F-Ratio
TOTAL	17	224.769	------	
Regression	1	229.954	229.954	248.33**
Residual	16	14.815	0.926	

Table 12. ANOVA for Eq. 15.

Source of Variation	Degrees of Freedom	Sum of Squares	Mean Square	F-Ratio
TOTAL	17	0.783	------	
Regression	1	0.593	0.593	49.83**
Residual	16	0.190	0.0119	

$\pm$ Two Standar Errors = $\begin{matrix} 1.65W_{50} \\ 0.61W_{50} \end{matrix}$

Table 13. ANOVA for Eq. 16.

Source of Variation	Degrees of Freedom	Sum of Squares	Mean Square	F-Ratio
TOTAL	17	58.368	------	
Regression	1	54.504	54.504	225.22**
Residual	16	3.864	0.242	

LIST OF REFERENCES

Anderson, R. C., "Distribution of the Serial Correlation Coefficient," The Ann. of Math. Stat., 8(1):1-13, March 1942.

Battan, Louis J., Radar Meteorology, Univ. of Chicago Press, 161 pp., 1959.

Britten, Margaret R., "Probability Analysis Applied to the Development of Synthetic Hydrology for the Colorado River," Bur. of Economic Research, Univ. of Colorado, 99 pp., October 1961.

Chow, Ven Te, Handbook of Applied Hydrology, McGraw-Hill, New York, 1420 pp., 1964.

Clark, Charles G. and Dooley, J. T., "Radar Data Acquisition Techniques," NSSL Rep. No. 24, U.S. Weather Bur., ESSA, Washington, D.C., pp. 122-130, August 1965.

Clark, R. A. and Moyer, V. E., "Some Theoretical Considerations of the Z-R Relationship," Proc. 12th Conf. on Radar Met., Norman, Oklahoma, pp. 245-249, October 1966.

Crawford, N. H. and Linsley, R. K., "The Synthesis of Continuous Streamflow Hydrographs on a Digital Computer," Tech. Rep. 12, Dept. of Civil Engineering, Stanford Univ., 121 pp., 1962.

Gray, Kathryn C. and Wilk, Kenneth E., "Data Processing at NSSL in 1964," NSSL Rep. No. 24, U.S. Weather Bur., ESSA, Washington, D.C., pp. 111-121, August 1965.

Harley, W. S., "An Operational Method for Quantitative Precipitation Forecasting," J. of App. Met., 4(3): 305-319, June 1965.

Hartley, H. O., "The Modified Gauss-Newton Method for the Fitting of Non-Linear Regression Functions by Least Squares," Technometrics, 3(2):269-280, May 1961.

Hartman, Monroe A., Ree, William O., Schoof, Russel R., and Blanchard, Bruce J., "Hydrologic Influences of a Flood Control Program," J. Hydraulics Div., ASCE, 93(3):17-25, May 1967.

Hiser, Homer W., "Type Distribution of Precipitation at Selected Stations in Illinois," Trans. Am. Geophys. Union, 37(4):421-424, August 1956.

Huddle, John P., "A Stochastic Technique for Synthesis of Hourly Precipitation," M.S. Thesis, Dep. of Met., Texas A&M Univ., 39 pp., May 1967.

Hudlow, Michael D., "Techniques for Hydrograph Synthesis Based on Analysis of Data from Small Drainage Basins in Texas," Water Resources Inst., Texas A&M Univ., 79 pp., 1966.

Huff, F. A., "The Adjustment of Radar Estimates of Storm Mean Rainfall with Rain Gage Data," Proc. 12th Conf. on Radar Met., Norman, Oklahoma, pp. 198-203, October 1966.

Imai, Ichiro, "Raindrop Size Distribution and Z-R Relationships," Proc. 8th Weather Radar Conf., San Francisco, pp. 211-218, 1960.

Johnson, Odell M., "Applicability of Radar Observations to the Prediction of Storm Runoff," M.S. Thesis, Dep. of Met., Texas A&M Univ., 37 pp., May 1967.

Johnstone, Don, and Cross, Williams P., Elements of Applied Hydrology, The Ronald Press Company, New York, p. 229, 1949.

Jones, Douglas M. A., "The Correlation of Rain-Gage Network and Radar-Detected Rainfall," Proc. 12th Conf. on Radar Met., Norman, Oklahoma, pp. 204-207, October 1966.

Julian, Paul R., "A Study of the Statistical Predictability of Stream-Runoff in the Upper Colorado River Basin," Bur. of Economic Research, Univ. of Colorado, 98 pp., October 1961.

Kessler, Edwin, "Radar Measurements for the Assessment of Areal Rainfall: Review and Outlook," Water Resources Research, 2(3):413-425, 1966.

Kessler, Edwin and Russo, J. A., "A Program for the Assembly and Display of Radar-Echo Distributions," J. of App. Met., 2(5):582-593, October 1963.

Laurenson, E. M., "Hydrograph Synthesis by Runoff Routing," Rep. No. 66, Water Research Lab., The Univ. of New South Wales, 248 pp., 1962.

Laurenson, E. M., "A Catchment Storage Model for Runoff Routing," J. of Hydrology, 2:141-163, 1964.

Levenberg, Kenneth, "A Method for the Solution of Certain Non-Linear Problems in Least Squares," Quar. of App. Math., 2:164-168, 1944.

Linsley, R. K., Kohler, M. A., and Paulhus, J. L. H., Hydrology for Engineers, McGraw-Hill, New York, 340 pp., 1958.

Marshall, J. S. and Palmer, W. McK., "The Distribution of Raindrops with Size," J. Met., 5(4):165-166, August 1948.

Minshall, Neal E., 1960, "Predicting Storm Runoff on Small Experimental Watersheds," J. Hydraulics Div., ASCE, 86(8):17-38, August 1960.

Parzen, Emanuel, Modern Probability Theory and Its Applications, John Wiley & Sons, Inc., New York, pp. 128-147, 1960.

Pattison, Allan, "Synthesis of Rainfall Data," Tech. Rep. No. 40, Dep. of Civil Engineering, Stanford Univ., 143 pp., July 1964.

Pattison, Allan, "Synthesis of Hourly Rainfall Data," Water Resources Research, 1(4):489-498, 1965.

Schreiber, H. R. and Kincaid, D. R., "Regression Models for Predicting On-Site Runoff from Short-Duration Convective Storms," Water Resources Research, 3(2): 389-395, 1967.

Shands, A. L. and Brancato, G. N., "Applied Meteorology: Mass Curves of Rainfall," Hydrometeorological Tech. Paper No. 4, Office of Hydrologic Director, U.S. Weather Bur., 56 pp., January 1947.

Sharp, A. L., Gibbs, A. E., Owen, W. J., and Harris, G., "Application of the Multiple Regression Approach in Evaluating Parameters Affecting Water Yields of River Basins," J. of Geophys. Research, 65(4):1273-1286, April 1960.

Soil Conservation Service, Engineering Handbook, Hydrology, Sup. A, Sect. 4: U.S. Dep. of Agr., Washington, D.C., pp. 3.15-1 to 3.15-7, 1957.

Stanton, Ralph G., Numerical Methods for Science and Engineering, Prentice-Hall, Inc., Englewood Cliffs, p. 84, 1961.

Tarble, Richard D., "The Use of Radar in Detecting Flood Potential Precipitation and Its Application to the Field of Hydrology," M.S. Thesis, Dep. of Met., Texas A&M Univ., 79 pp., May 1957.

Teague, Jack L., "The Use of Radar in Flash Flood Forecasting," S. Reg. Tech. Memorandum No. 23, RFC, U.S. Weather Bur., ESSA, Fort Worth, Texas, 31 pp., August 1966.

Thomas, H. A., Jr. and Fiering, M. B., Design of Water-Resource Systems: Chap. 12, Harvard Univ. Press, Cambridge, pp. 459-493, 1962.

U.S. Dept. of Ag., Soil, The 1957 Yearbook of Ag., U.S. Gov. Printing Off., Washington, D.C., 784 pp., 1957.

Wilson, James E., "Evaluation of Precipitation Measurements with the WSR-57 Weather Radar," J. of App. Met., 3(2):164-174, April 1964.

Wilson, James E., "Storm-to-Storm Variability in the Radar Reflectivity-Rainfall Rate Relationship," Proc. 12th Conf. on Radar Met., Norman, Oklahoma, pp. 229-233, October 1966.